CHAPTER

THE SAKATTI CU-NI-PGE SULFIDE DEPOSIT IN NORTHERN FINLAND

3.7

W. Brownscombe, C. Ihlenfeld, J. Coppard, C. Hartshorne, S. Klatt, J.K. Siikaluoma, R.J. Herrington

ABSTRACT

The Sakatti Cu-Ni-PGE sulfide deposit was discovered by Anglo American in northern Finland in 2009. It consists of both disseminated and massive sulfides, hosted by a large olivine cumulate body, surrounded by volcanic rocks that make up the footwall and part of the hanging wall. A polymict breccia constitutes the majority of the hanging wall. Two smaller satellite olivine cumulate bodies also host mineralization. The sulfide mineralization is generally Cu-dominated, especially in the shallower part of the deposit, with a transition to more Ni-rich and Ni-dominated mineralization in its deeper part. Disseminated mineralization is only found within the olivine cumulate bodies, whereas massive sulfides extend up to 150 m into the footwall, where they rapidly evolve toward very low Ni/Cu ratios.

Keywords: Sakatti; Ni-Cu-PGE; magmatic sulfide; ultramafic; nickel; olivine cumulate.

INTRODUCTION

Sakatti is one of only a handful of significant Ni-Cu sulfide deposits discovered globally in the past decade, and is one of the most significant discoveries in Finland for more than a generation. The deposit was discovered during a regional Ni sulfide exploration program initiated by Anglo American in Fennoscandia in 2002 under the leadership of Jim Coppard.

In this chapter, the main features of the Sakatti deposit are presented and the current level of understanding is briefly explored. The information presented extends up to the time of writing but inevitably, with a relatively recent discovery, there is significant uncertainty and also a large amount of evidence and information still to be discovered. The deposit is located within the Central Lapland Greenstone Belt (CLGB), which extends across Lapland from northern Norway to the Finnish–Russian border (Fig. 3.7.1). The CLGB contains numerous ultramafic intrusive and extrusive bodies and, following the Sakatti discovery, can be viewed as being highly prospective for Ni-Cu sulfide deposits.

DISCOVERY HISTORY

Nickel sulfide exploration across Fennoscandia by Anglo American began in 2002. Initial tenure applications in the region were made in 2003 over mapped mafic–ultramafic sills intruded within the outlines of the Central Lapland Greenstone Belt (CLGB). The high-quality Aeromagnetic and Frequency

Mineral Deposits of Finland. http://dx.doi.org/10.1016/B978-0-12-410438-9.00009-1

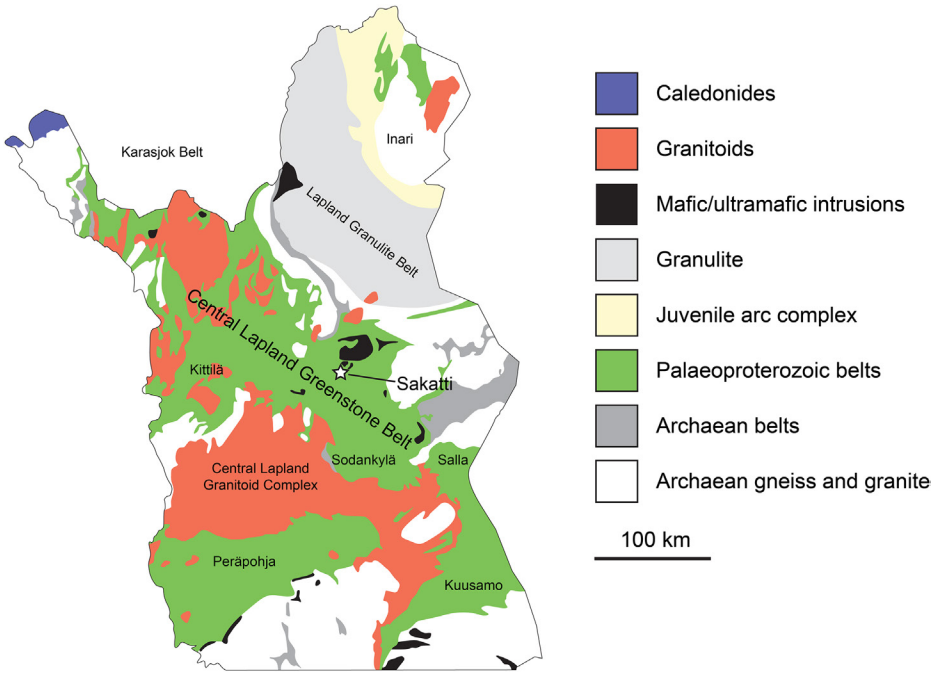

FIGURE 3.7.1 Regional map of the CLGB showing the location of the Sakatti deposit.

Source: *After Hanski and Huhma (2005).*

Electromagnetic (AMFEM) dataset (200 m line spacing, 30 m altitude) of the Geological Survey of Finland (GTK) covering the whole region was the primary base dataset used in initial target generation. Combined with the public domain digital geological maps and geochemical data from GTK, the AMFEM data enabled an initial prioritization of targets, with Sakatti chosen as target number eight (MOS8) on the first day of detailed targeting. At that time, the base datasets used had been in the public domain for more than a decade.

The initial targets were subsequently followed up by ground geophysical methods and soil geochemistry. An infill GTK AMFEM survey was later carried out to provide 100-m line spacing. This was done to better define the priority targets and to generate additional targets within the region. With processing of the wing-tip sensors, this produced an effective 75 m line spacing coverage of the area of exploration interest. The exploration methodologies were continuously adapted and improved until an effective system had been developed. It was apparent from geochemical orientation surveys conducted during the first field season that surface soil geochemistry was ineffective due to a number of reasons, including complex ice flow directions, multiple till layers, and airborne pollution from the Norilsk Nickel smelter at Nikel in Russia. Base of till (BOT) geochemistry, which involves the collection of till samples at the till–bedrock interface, proved to be the most effective geochemical tool.

Initial drill testing of Sakatti started in the late spring of 2006 when three diamond drill holes (DDH) were drilled at the eastern edge of the magnetic anomaly. Borehole DDH 06MOS08003 returned a number

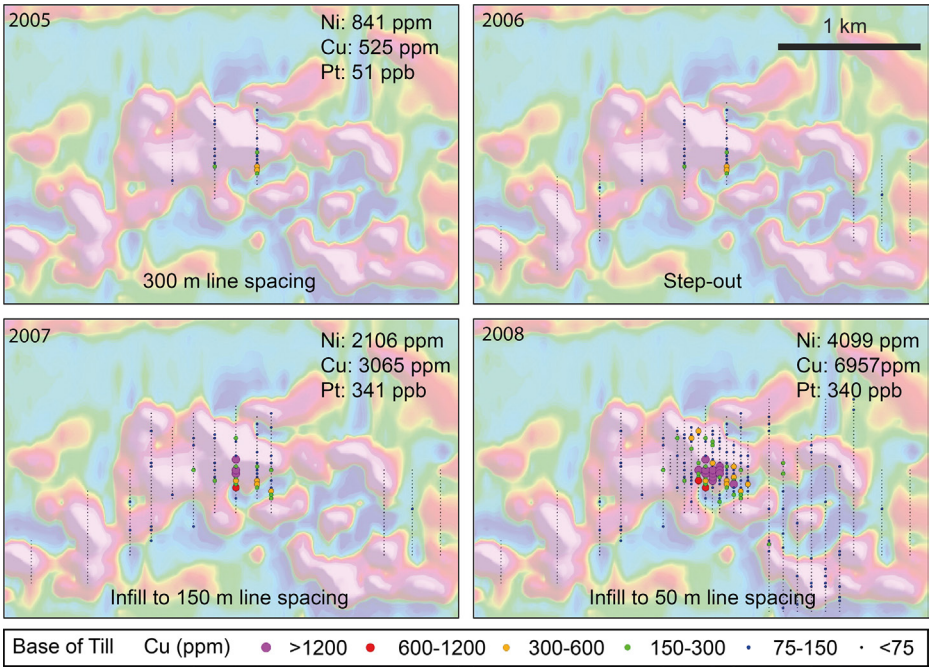

FIGURE 3.7.2 Base-of-till geochemistry undertaken over the Sakatti deposit prior to discovery, overlain on an airborne magnetic map (reduced to pole).

The base-of-till anomaly was well defined by 2008 and was approximately 150 m × 150 m. Given values refer to the highest Cu sample in each year.

of short significant intervals of Cu-PGE[1]-Au mineralization but with only background Ni. Importantly, the DDH was abandoned within the olivine cumulate due to the beginning of the spring thaw, when ground conditions became unstable. A year-end review of the 2006 field program by Anglo American's internal and external nickel commodity experts severely downgraded the Sakatti target and all work on it ceased.

An exploration review in 2007 within the Finland office team highlighted once again the potential of Sakatti and a detailed BOT grid was undertaken (Fig. 3.7.2) with resources diverted from other targets and projects within Fennoscandia. This detailed BOT geochemistry program returned highly significant coherent and coincident Ni, Cu, and PGE anomalies with values up to 6957 ppm Cu, 5575 ppm Ni, and 739 ppb Pt over the sub-cropping portion of the Sakatti deposit (Fig. 3.7.2).

Funding to continue the program was secured from senior management in London, and a second drill phase commenced in the winter of 2008, when the first important disseminated and minor vein-related mineralization was intersected in DDH 08MOS08007. This phase of exploration highlighted the economic potential of Sakatti. The official discovery borehole at Sakatti was DDH 09MOS08013, drilled in 2009. It intersected 110.00 m at 1.3 wt% Cu, 0.2 wt% Ni, 0.5 g/t Pt, 0.3 g/t Pd, and 0.4 g/t Au. This DDH proved that Sakatti is a significant mineralized system.

[1] PGE = platinum-group elements (Pt, Pd, Rh, Ir, Os, and Ru).

The GTK AMFEM and Geotech VTEM (Versatile Time Domain Electromagnetic) airborne survey systems flown over the Sakatti area do not show a recognizable geophysical response over the main cumulate body at Sakatti, but highlight the smaller, structurally offset, northeast and southwest satellite bodies. The northeast body consists of a similar style of mineralization to the main body and drilling has intersected two massive sulfide lenses (e.g., DDH 12MOS08079 with 39.95 m at 3.40 wt% Cu, 3.54 wt% Ni, 1.81 g/t Pt, 2.09 g/t Pd, and 0.45 g/t Au). The southwest body includes sub-cropping, weathered massive sulfides, and deeper, unweathered massive sulfides.

Due to the depth (>350 m), the highly conductive nature and interconnectedness of the massive and vein-style sulfide mineralization in the main body, very late-time channel responses are required to detect the deposit. With conventional electromagnetic geophysical techniques the noise level overpowers the response in these very late-time channels. In contrast, Anglo American's in-house low-temperature superconducting quantum interference device (LTSQUID) TEM (Transient Electromagnetic) system returned clean late-time responses over Sakatti, and with hindsight, the modeled results were remarkably accurate. In addition, the magnetic anomaly at Sakatti is now known to be a response of the serpentinization of the peridotite and is not related to the mineralization itself.

GEOLOGICAL SETTING

The Sakatti deposit is located within the Paleoproterozoic Central Lapland Greenstone Belt (CLGB), a complex succession of sedimentary and volcanic rocks, with the latter ranging from komatiitic to rhyolitic in composition. The evolution of the CLGB spans about 600 Ma starting with andesitic volcanism at ~2.5 Ga and ending with deposition of molasse-type coarse clastic sediments at <1.9 Ga. The belt is also host to several mafic–ultramafic intrusions, including the 2439 ± 3 Ma Koitelainen layered intrusion and the 2058 ± 4 Ma Kevitsa intrusion (Mutanen and Huhma, 2001). The geology of this area is exceptionally well described in publications by GTK. A comprehensive summary of this work is given in Hanski and Huhma (2005).

The stratigraphic level at which Sakatti was located within the CLGB has not yet been resolved, as the units so far intersected do not correspond conclusively to any particular part of the CLGB succession. On a regional scale, the deposit is surrounded by pelitic metasediments of the Matarakoski formation and quartzites of the Sodankylä group, which were deposited between ~2.3 and 2.06 Ga. However, neither of these rock formations has been identified in drill core at Sakatti. It is interesting to note in this context that the Ni-Cu ore-bearing Kevitsa intrusion, which is located approximately 15–20 km northeast of Sakatti, was emplaced in mica schists and black schists of the Matarakoski formation.

DEPOSIT OVERVIEW

Based on current understanding, the Sakatti deposit consists of three spatially distinct mineralized bodies of olivine cumulate named "main body," "northeast body," and "southwest body" (Fig. 3.7.3). Mineralization in each of the three is hosted within or at a basal contact of the olivine cumulate. In hand specimens, there are no discernible petrological differences between these three bodies.

The major host and wall rock units of the deposit comprise the *peridotite unit, aphanitic unit, mafic suite, breccia unit* and *volcaniclastic unit*. These units are defined in the following and their relationship is illustrated later in Figs. 3.7.5, 3.7.6, and 3.7.7. The composition and location of these units are

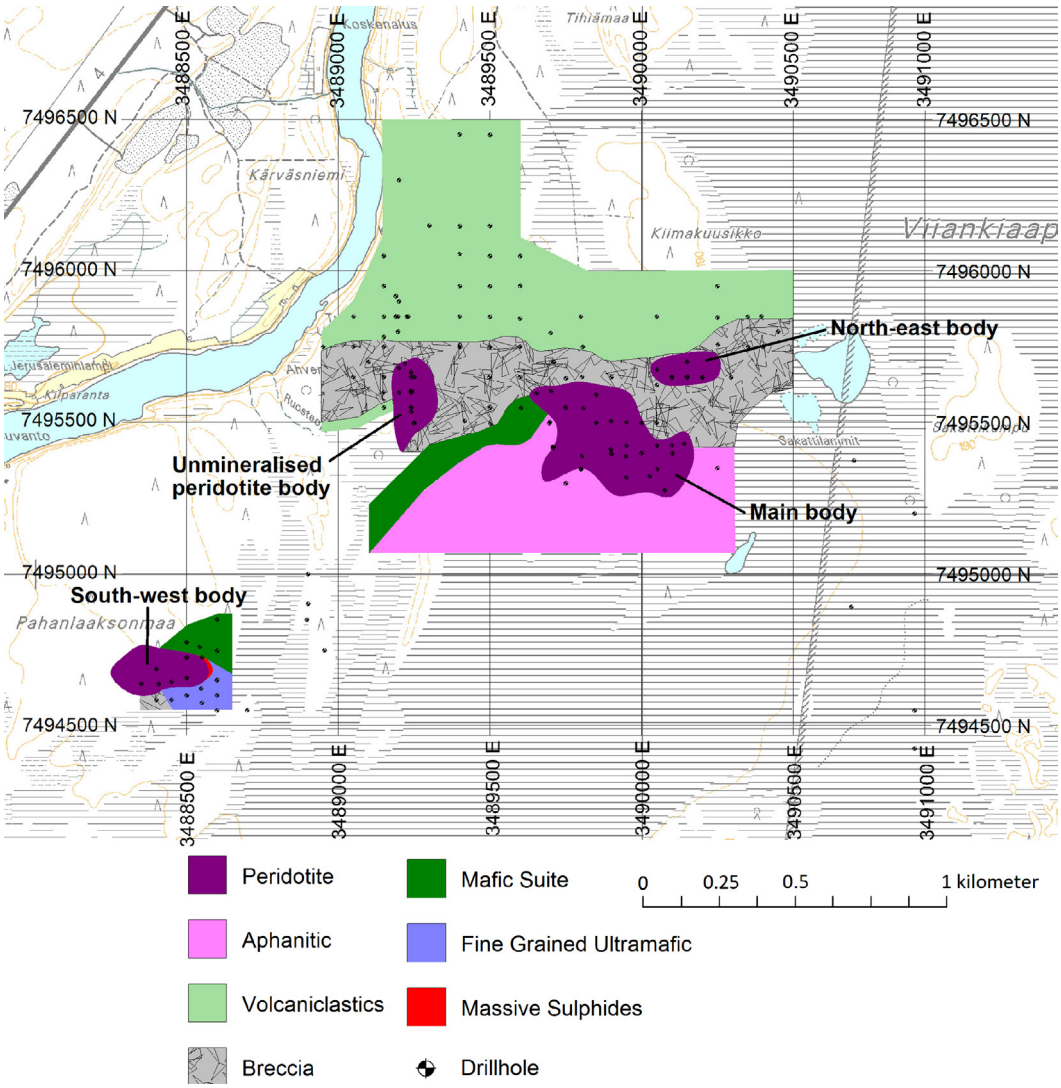

FIGURE 3.7.3 Plan map of the Sakatti deposit showing the interpreted geology and drill hole locations.

The horizontal lines indicate wetland.

briefly described in this section and their mineralogical and chemical compositions are discussed in more detail in the "Petrology and geochemistry" section later in the chapter.

KEY LITHOLOGIES

Peridotite unit

This is an olivine cumulate with variable oikocrystic pyroxene content and rare minor interstitial plagioclase. The peridotite unit is the principal constituent of the main cumulate body, which itself

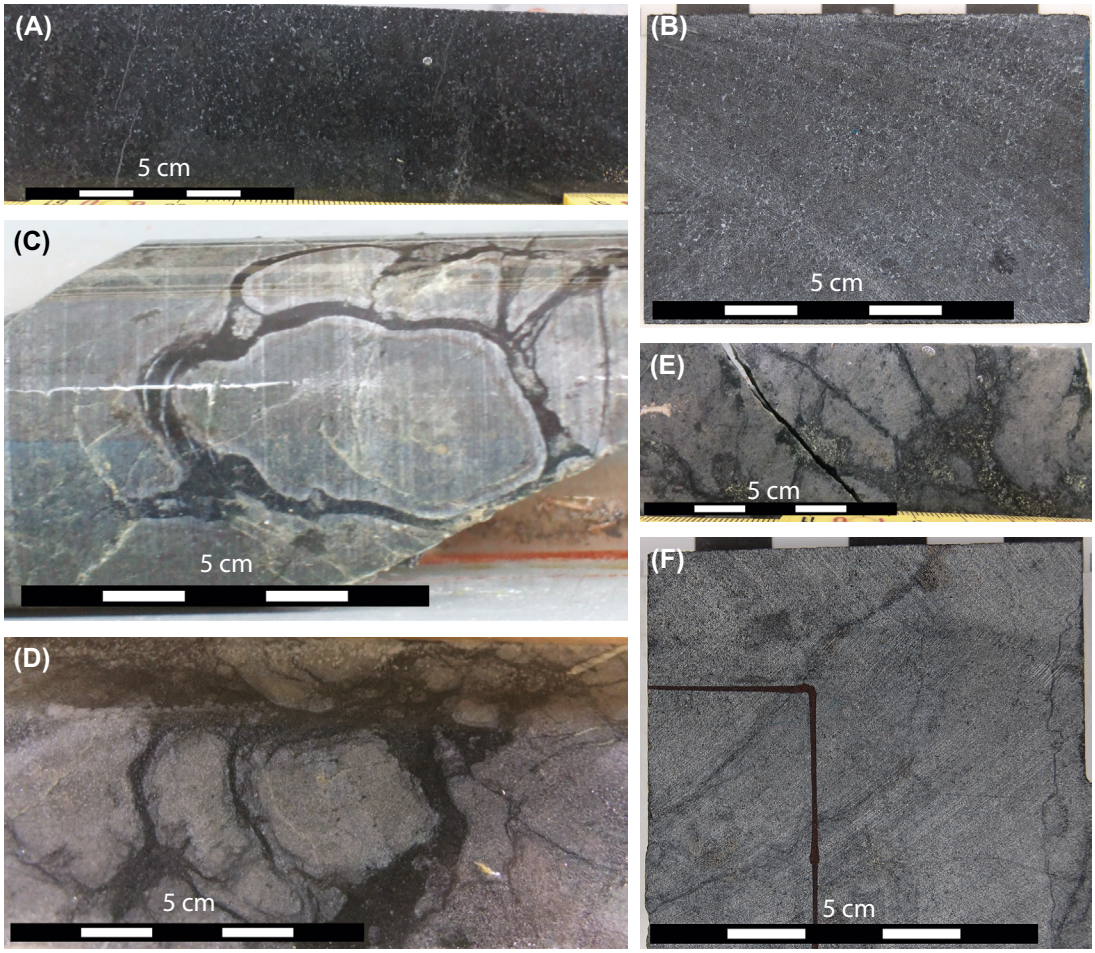

FIGURE 3.7.4 Photographs of drill core from the Sakatti deposit.

(A,B) Typical peridotite from the main cumulate body; (C,D) typical samples of the aphanitic unit in contact with the cumulate body; (E) aphanitic unit intruded by mineralized peridotite of the main body; (F) aphanitic unit that is located more than 100 m from the cumulate body.

can be more than 400-m thick. Most of the unit is pervasively serpentinized, and should technically be termed a serpentinite. However, the cumulate texture is preserved (Fig. 3.7.4(A) and (B)), and therefore the rock can be considered in terms of its protolith. Textures within the main body range from adcumulate to orthocumulate with the groundmass typically also composed of serpentine with minor talc.

The *altered ultramafic* is a logging unit interpreted to be a talc-carbonate alteration product of the peridotite. This unit is invariably present where the peridotite is in direct contact with the overlying breccia unit. The *dunite* is another logging subunit of the peridotite. It is an olivine adcumulate marked

by an almost complete lack of serpentinization and forms a continuous, discrete package at the base of the peridotite in the northwestern part of the main body. Primarily in the upper part of the peridotite unit, coarse, *pegmatoidal gabbro* may occur. These rocks display sharp contacts with peridotite and comprise intersections of between 50 cm and 15 m.

Aphanitic unit

The aphanitic unit, so named because of its grain size and likely volcanic origin, forms the hanging wall, footwall, and sidewall to much of the main cumulate body, notably along the southern edge and the far western side. Referring to a unit as aphanitic is clearly problematic as it is not an adequate rock name. This name has endured because the unit has proved difficult to classify. The mineralogical and textural features of this unit all point toward a volcanic origin.

The rock is classified as a plagioclase-rich picrite with 10–15% small (<0.5 mm) phenocrysts of olivine and minor plagioclase (up to 1 mm) in a fine-grained groundmass of plagioclase, pyroxene, and minor olivine. Where it is within 50 m of the contact with the peridotite unit, the aphanitic unit exhibits an unusual texture containing injections of the peridotite unit (Fig. 3.7.4(C), (D), and (E)). Further from the contact, this texture is not present and the rocks merely show serpentine veining (Fig. 3.7.4(F)).

The *footwall mafic rock* is a logging unit referring to what is interpreted as an alteration product of the aphanitic unit. The rock consists mainly of chlorite, phlogopite, and talc, accompanied by carbonate veins and fracture fill.

Mafic suite

In addition to the aphanitic unit, the hanging wall of the Sakatti deposit contains several other lithological units, including the mafic suite. It is present in the southwestern part of the deposit where it occurs between the peridotite or aphanitic units and the breccia unit. It comprises three separate logging units: the *mafic volcanic rock, the scapolite-mica rock* and the *hanging-wall gabbro*. The mafic volcanic rock is a strongly chlorite-amphibole-altered lithology that, when in close proximity to the breccia unit, has undergone in situ brecciation and precipitation of matrix and vein calcite. The scapolite-mica rock is a strongly foliated, almost schistose rock with a biotite matrix hosting scapolite porphyroblasts. The hanging-wall gabbro comprises a series of gabbroic sills that intrude the mafic volcanic and scapolite-mica rocks but do not intrude the main cumulate body. At the contact between the scapolite-mica rock and the aphanitic unit, a cryptocrystalline *serpentinite unit* is frequently present.

Breccia unit

The breccia unit is a 100–300-m-thick hematite-dolomite-albite-talc altered, and exceptionally heterogeneous, polymict breccia package that lies stratigraphically above the main cumulate body. Various zones can be differentiated within the breccia unit, including zones with predominant albite or carbonate (calcite/dolomite) alteration, as well as polymict zones where rounded to angular clasts of talc, chlorite, and quartz typically occur in a calcite matrix.

Volcaniclastic unit

The volcaniclastic unit is the stratigraphically uppermost unit in the hanging wall of the Sakatti deposit. It is a phyllite with biotite porphyroblasts and a crenulation cleavage throughout. It is interpreted as a metamorphosed volcano-sedimentary package. The thickness of this unit is at least 600 m.

Footwall units

In the eastern part of the deposit, where the aphanitic unit forms the primary footwall below the peridotite unit, a clay-rich zone, interpreted as a fault structure, is present beneath the aphanitic unit. In the west, this fault structure occurs directly at the base of the peridotite unit and has often necessitated the cessation of drilling. Beneath this fault, a strongly laminated carbonate-rich metasediment is present. No sulfides have been observed in this metasediment.

MORPHOLOGY OF THE SAKATTI DEPOSIT

Main cumulate body

The northwest-plunging main cumulate body is by far the largest of the three cumulate bodies (see Fig. 3.7.3), with a currently delineated extent of more than 1100 m down-plunge from surface to a depth of 1220 m below surface, and a maximum thickness of more than 400 m. The cumulate body is roughly tubular, yet irregular in shape, with a shallower plunge near surface in the east and at depth in the north and west. These two shallowly plunging parts are connected by a more steeply plunging north-northwest to south-southeast orientated part of the body (Fig. 3.7.5).

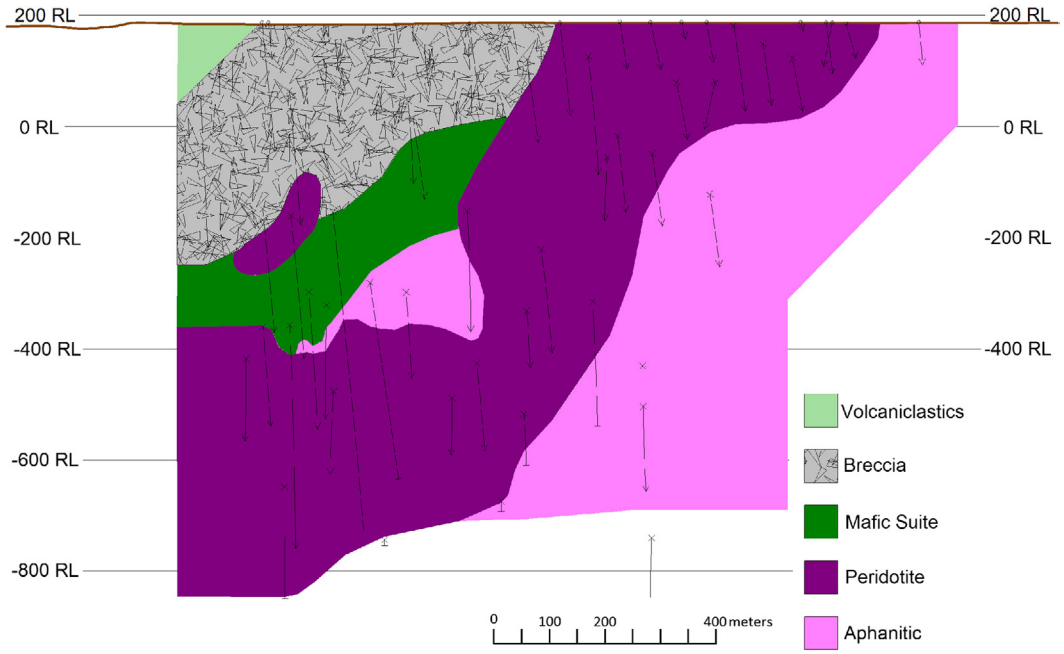

FIGURE 3.7.5 West-northwest to east-southeast angled section, ±25 m clipping, through the main body of the Sakatti deposit at 110° through center point 3489600E 7495600N.

This shows the changing geometry of the cumulate body and the crosscutting relationship of the cumulate with both the mafic suite and the aphanitic unit. Boreholes intersecting the 50 m wide section are shown as lines, with cross and arrows indicating where they enter and leave the section or crossbars where they terminate within the section.

Broadly speaking, the main cumulate body occurs stratigraphically below the breccia unit but above the aphanitic unit; however, the exact stratigraphic setting is locally more complex. The geology in the eastern portion of the main body is relatively simple (Fig. 3.7.6). The peridotite subcrops beneath the glacial till cover, and a mixture of aphanitic and altered aphanitic rocks form the southern sidewall and basal contact to the cumulate body.

With increasing depth further to the west, an extensive package of nonmineralized hanging wall rocks is encountered before reaching the cumulate body (Fig. 3.7.7). In this western part of the deposit,

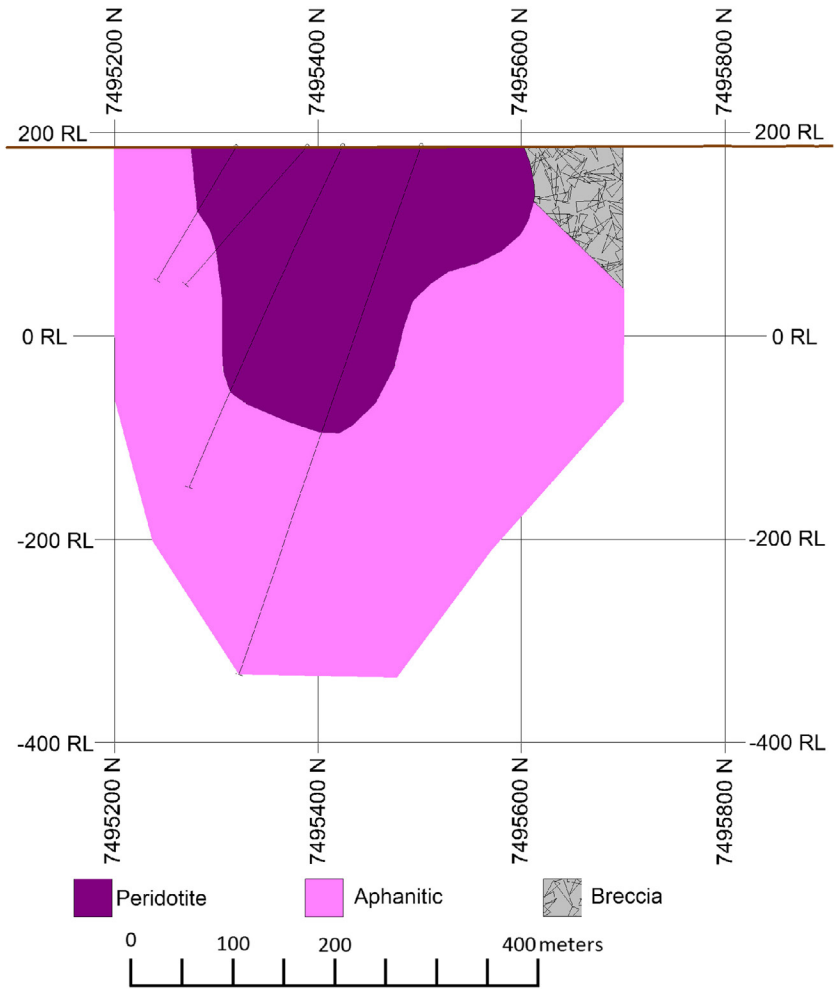

FIGURE 3.7.6 South to north cross section, ±25 m clipping, through the main body of the Sakatti deposit on 3489950E.

This shows the aphanitic footwall surrounding the main cumulate body and a small portion of the hanging-wall breccia. Boreholes intersecting the 50 m wide section are shown as lines, with cross and arrows indicating where they enter and leave the section or crossbars where they terminate within the section.

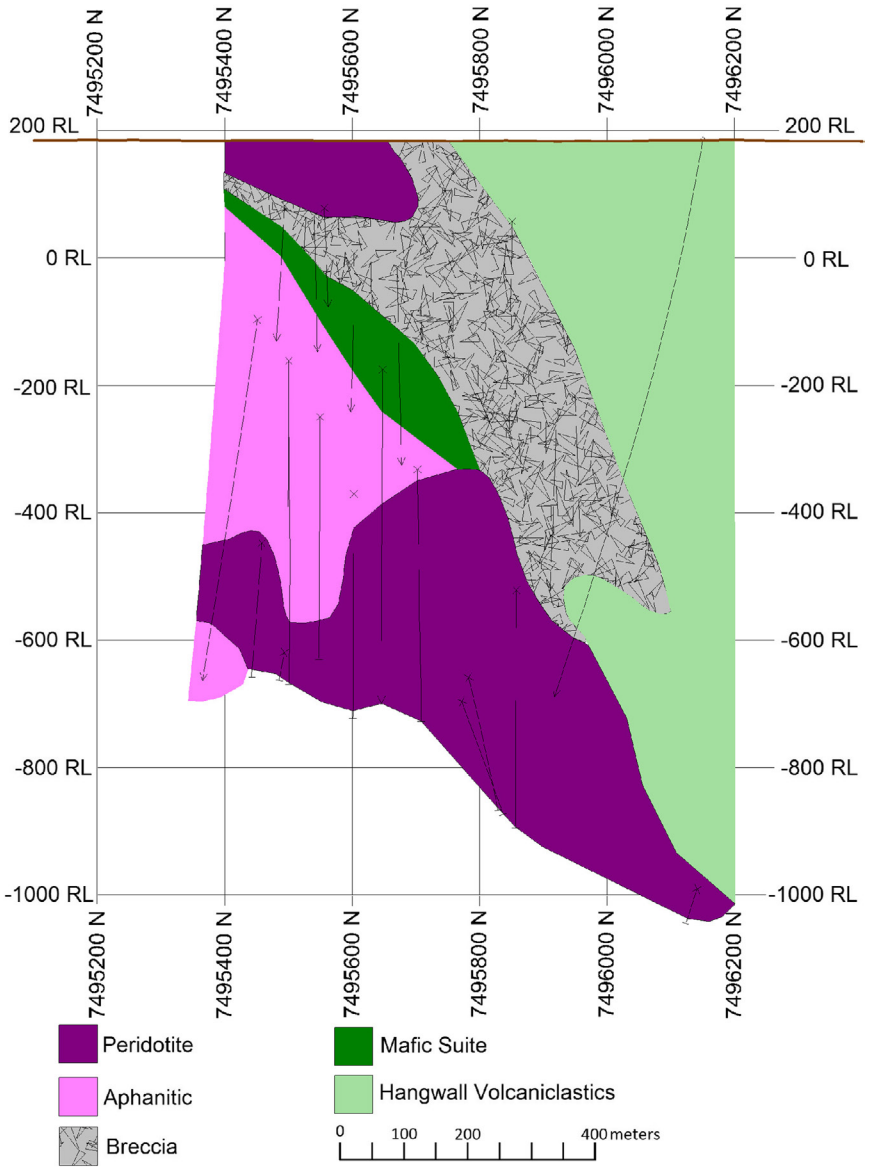

FIGURE 3.7.7 South to north cross section, ±25 m clipping, through the main body of the Sakatti deposit on 3489300E.

The hanging wall contains volcaniclastics, breccia, the mafic suite, and an unmineralized peridotite. The aphanitic unit is present both above and below the peridotite unit. The base of the cross section is a faulted contact. Boreholes intersecting the 50 m wide section are shown as lines, with cross and arrows indicating where they enter and leave the section or crossbars where they terminate within the section.

the aphanitic unit constitutes both the hanging wall and part of the footwall of the cumulate body (the remainder of the footwall is a fault structure).

The upper contact of the aphanitic unit with the remainder of the hanging wall is always marked by a cryptocrystalline serpentinite unit. Stratigraphically above the aphanitic unit and the serpentinite is the northwest-dipping mafic suite. Above this package is the breccia unit, which also dips to the northwest and appears to be concordant with the underlying mafic suite. Toward the north, the package of aphanitic unit, serpentinite, and mafic suite pinches out and the cumulate body is in direct contact with the breccia unit. Further to the north, the breccia unit itself pinches out to leave the volcaniclastic unit in contact with the cumulate body. An apparently isolated nonmineralized peridotite cumulate body subcrops at surface within the breccia unit in this western portion (see Fig. 3.7.7), without any established links to the main cumulate body.

Northeast cumulate body

Based on the evidence of current drilling, the northeast cumulate body is smaller than the main cumulate body and more cylindrical, albeit with an elongate tail to depth, giving it an inverted teardrop-like shape (Fig. 3.7.8). It has a west–east strike and gently plunges to the east. It occurs at a different stratigraphic level to the main cumulate body, as it is bound by the volcaniclastic unit to the north and the breccia unit to the south and at depth.

Talc-carbonate-altered ultramafic rocks are also more common when compared to the main cumulate body, particularly to the east. In the west, a 20–30-m-thick cryptocrystalline serpentinite body occurs within the peridotite, almost perpendicular to the contact between the cumulate body and the volcaniclastic unit. Only one drill hole has extended from the northeast cumulate body toward the main cumulate body and this hole intersected a fault at depth.

Southwest cumulate body

The southwest cumulate body is ovoid in shape, with a central sub-cropping portion and a gently dipping eastern edge. The western edge is untested by drilling. Scapolite-mica rock occurs to the north of the cumulate body, and a breccia occurs at depth and to the south. At surface in the southeast is a fine-grained, amphibole-rich, ultramafic rock that has not been intercepted elsewhere within the Sakatti area.

MINERALIZATION

Mineralization at Sakatti consists of disseminated, vein, semi-massive, and massive sulfides (Fig. 3.7.9). Vein, semi-massive, and massive mineralization is found mostly within the olivine cumulate bodies but can extend into the aphanitic footwall and hanging wall. In contrast, the disseminated mineralization is only found within the olivine cumulate bodies. Not all of the main cumulate body is mineralized; within the relatively thick central and eastern portions of the body, typically only the bottom half hosts mineralization. In the far west and north where the cumulate body is relatively thin, mineralization occurs throughout the entire cumulate package.

Main body

The massive sulfide mineralization is present within the peridotite and also extends into the aphanitic footwall and sidewall of the peridotite for up to approximately 150 m. There are several different lenses of massive sulfides, at least two of which can be correlated between drill holes. The lenses are thickest

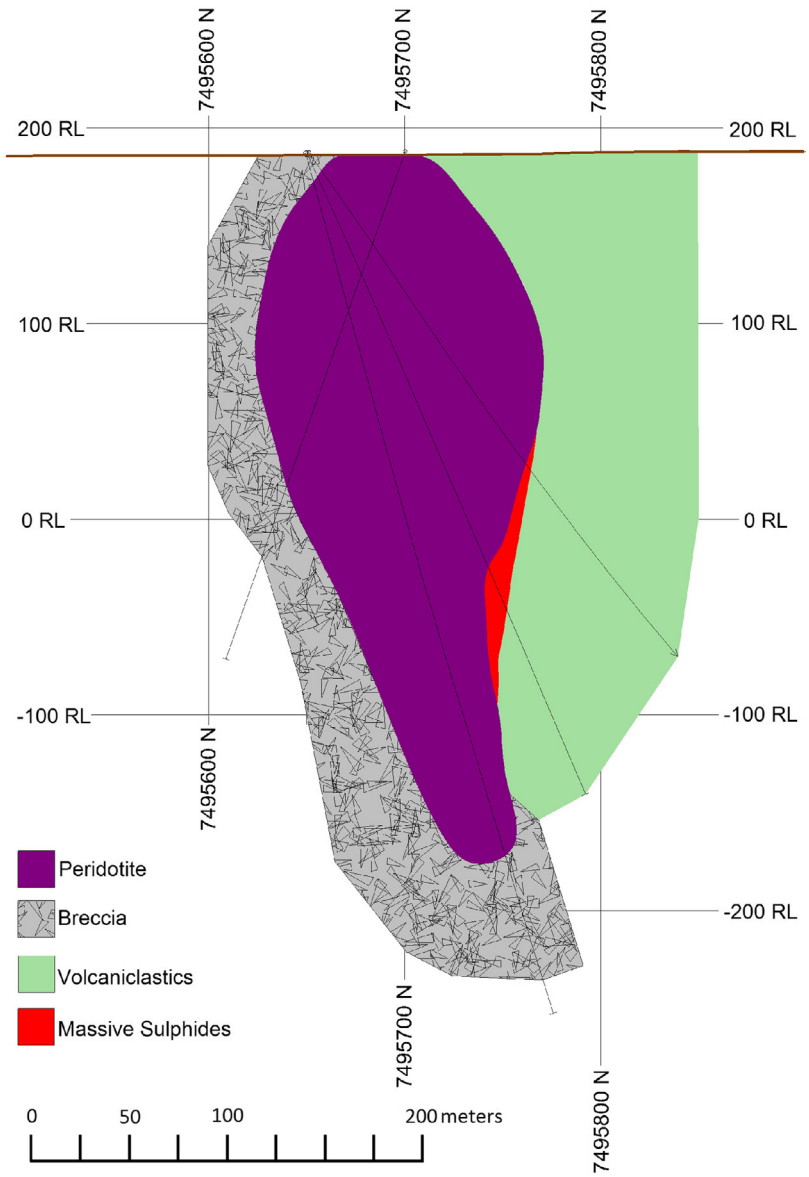

FIGURE 3.7.8 South to north cross section through the northeast body of the Sakatti deposit on 3490150E.

Peridotite occurs between breccia and volcaniclastics. Boreholes intersecting the 50 m wide section are shown as lines, with cross and arrows indicating where they enter and leave the section or crossbars where they terminate within the section. Solid lines represent boreholes.

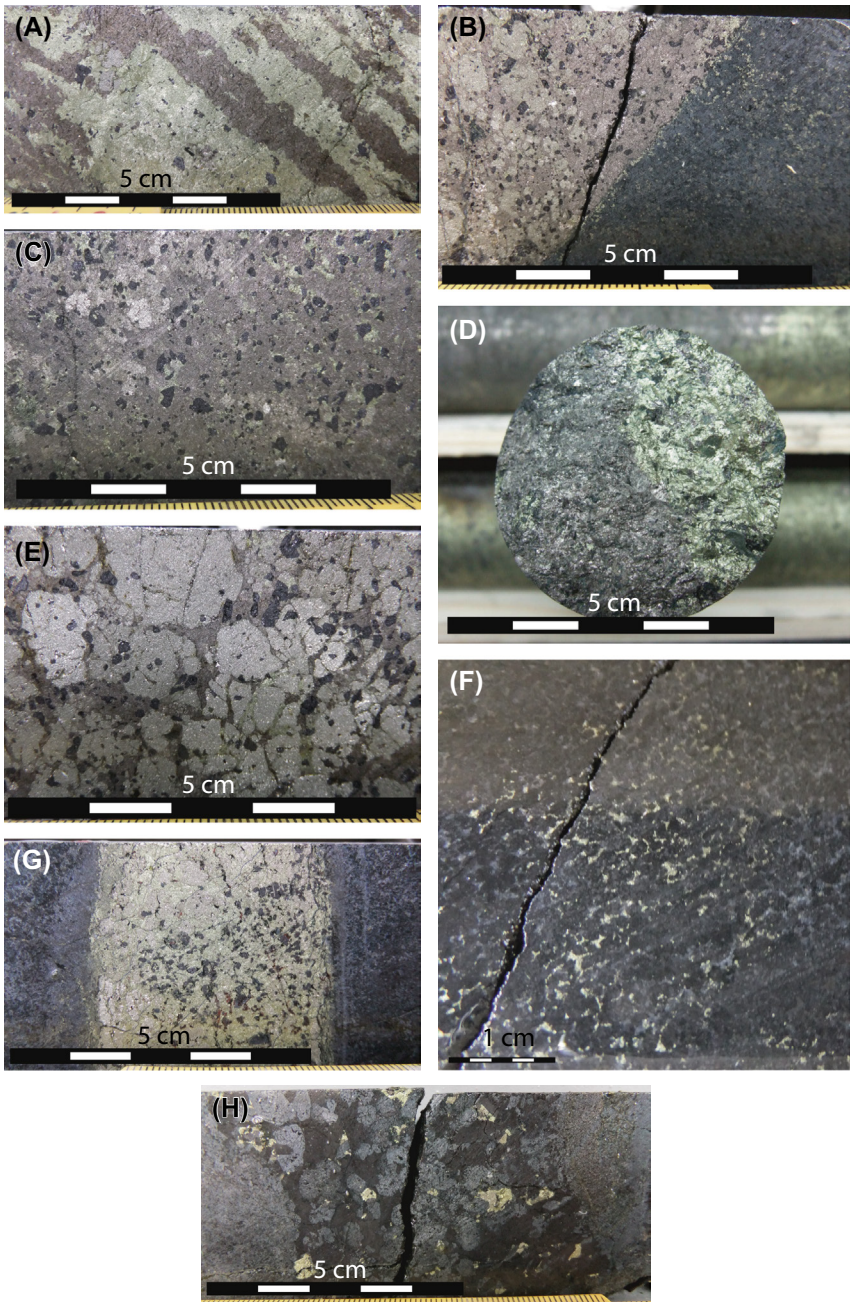

FIGURE 3.7.9 Photographs showing Ni-Cu sulfide mineralization in drill core from the Sakatti deposit.

(A) Chalcopyrite-dominated massive sulfide mineralization with streaks of pyrrhotite and minor pentlandite and magnetite; (B) contact of pyrrhotite-pentlandite-pyrite massive sulfide mineralization with olivine cumulate; (C) pyrrhotite-pentlandite massive sulfides with minor chalcopyrite and euhedral magnetite; (D) massive sulfides showing segregation of pyrrhotite-pentlandite and chalcopyrite; (E) pyrite style of mineralization characterized by large pyrite grains typical of, but not exclusive to, the northeast body mineralization; (F) typical chalcopyrite-dominated disseminated/interstitial mineralization; (G) chalcopyrite- and pyrite-rich vein-style of mineralization; (H) semi-massive mineralization hosted by pegmatoidal gabbro.

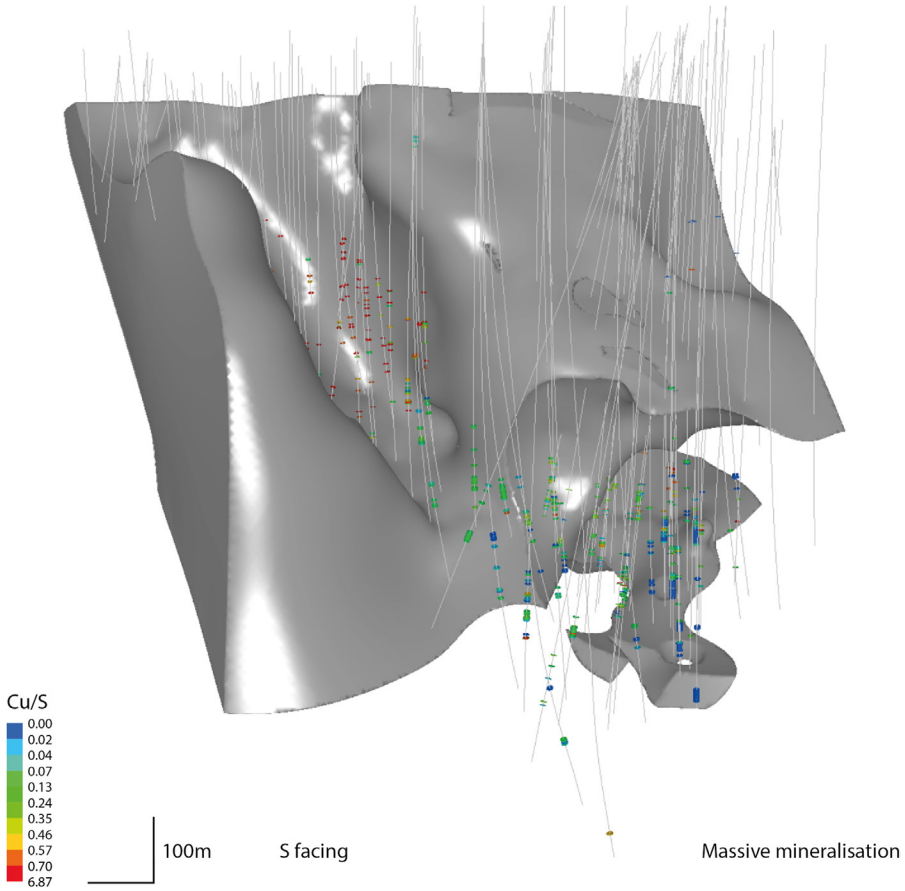

FIGURE 3.7.10 3D diagram showing Cu-S ratios for intersections of massive sulfides in the Sakatti deposit.

The upper contact of the aphanitic unit is shown in gray and the peridotite unit has been removed. Solid lines represent boreholes.

(up to 25 m) in the center of the deposit and thin out to as little as 0.5 m toward both the northwest and southeast.

The massive and veined sulfide mineralization within the main cumulate body shows a distinct fractionation in Ni-Cu ratios. In the west and northwest (i.e., in the deeper portions of the deposit) massive sulfides are composed of pyrrhotite-pentlandite-chalcopyrite with overall Ni-Cu ratios greater than one. The composition of the massive sulfides evolves up-plunge to become increasingly chalcopyrite-dominated (Fig. 3.7.10).

Massive sulfide lenses extending from the cumulate body into the aphanitic unit show decreasing thickness and Ni-Cu ratios with distance from the cumulate body, but these trends occur over a much shorter distance than those observed up-plunge within the cumulate body. At the terminal extremities

of the massive sulfide lenses, both within the cumulate body and the aphanitic unit, there is a marked increase in precious metal tenors, in particular that of Pt.

An additional style of mineralization is typified by coarse, pegmatoidal gabbroic silicates with semi-massive sulfides (Fig. 3.7.9(H)). The coarse, pegmatoidal gabbroic subunit occurs both with and without associated sulfide mineralization.

Vein sulfides are present to a lesser extent throughout the main peridotite cumulate body, but are most abundant in its shallow southeastern part where the massive sulfide lenses show relatively low Ni-Cu ratios and reduced thickness. The sulfide veins are mostly relatively thin with a broad range of orientations and contain predominantly chalcopyrite. As such, they are judged to be distinct from the massive sulfides. The veins are generally 5–20 cm thick, but can be up to 50 cm in thickness. The use of the term "vein" is not intended to imply an epigenetic hydrothermal origin; rather, the veins are interpreted to represent fractionated apophyses of the main massive sulfide lenses.

Disseminated sulfides or the interstitial mineralization, as it is commonly called, occur predominantly in the central, steeply plunging and the southeast, shallowly plunging parts of the main cumulate body. In terms of composition, the mineralization is generally chalcopyrite-dominated with only minor pyrrhotite, pentlandite, and pyrite. The occurrence of this style of mineralization is spatially independent of the other styles. In many places the disseminated mineralization is cut by massive sulfide veins of varying composition and size. However, there are numerous examples where disseminated sulfides show no spatial association with massive sulfides, either vertically or laterally. This is especially the case at depth in the northwestern part of the body.

The disseminated sulfides are generally chalcopyrite-dominated but the Cu-S ratio shows considerable variation, being relatively Cu-poor in the deeper northwestern part of the main body and relatively Cu-rich in the shallow southeastern part (Fig. 3.7.11). As discussed in greater detail later in this chapter, minor interstitial chalcopyrite also occurs in small peridotitic intrusions within the hanging wall and footwall aphanitic unit, although this is restricted to within 20 m of the contact with the cumulate body.

Northeast body

Mineralization in the northeast body is almost entirely limited to massive sulfides at the basal contact between the cumulate body and the volcaniclastic package. Disseminated mineralization is of minor significance.

The metal tenors of the massive sulfides are very similar to those of massive sulfides at depth in the main cumulate body; Ni contents are roughly equal to or greater than Cu contents, and Pt and Pd are present in a ratio of 2:1, although both Pt and Pd are enriched compared to massive sulfides in the main cumulate body. One notable difference when compared to the main body is the abundance of coarse-grained pyrite and the lack of pyrrhotite.

Southwest body

Mineralization in the southwest cumulate body occurs in a variety of forms. On the eastern side of the body, mineralization is massive and semi-massive and located within chlorite gouge at the upper contact of the cumulate. Moving further west, massive sulfides and semi-massive sulfides, as well as clasts of massive sulfide, are found within the body. All mineralization in the southwest body is Ni-dominated with a Ni-Cu ratio of 2.

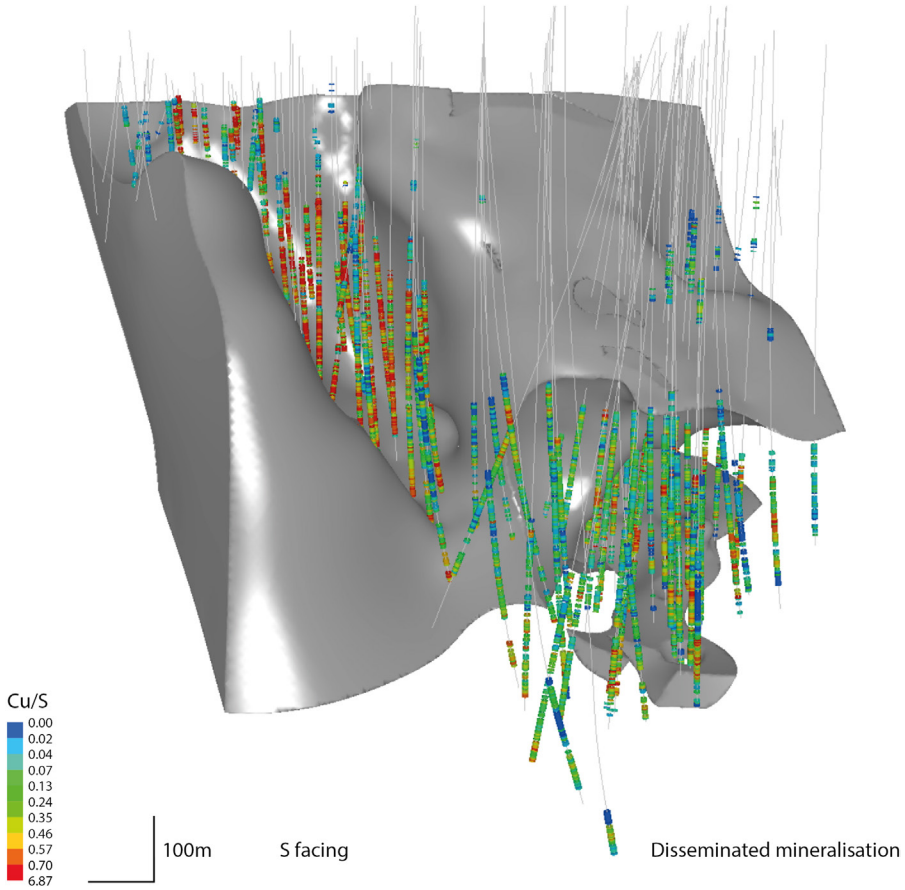

FIGURE 3.7.11 3D diagram showing Cu-S ratios for intersections of disseminated sulfides in the Sakatti deposit.

The upper contact of the aphanitic unit is shown in gray and the peridotite unit (where mineralization occurs) has been removed.

PETROLOGY AND GEOCHEMISTRY

Investigation of the lithologies of the Sakatti deposit beyond hand specimen identification has involved a variety of techniques, relying primarily on conventional thin section microscopy and whole-rock geochemistry. In addition, the mineral chemistry of preserved magmatic minerals has been extensively investigated to constrain the petrogenesis of the deposit.

PERIDOTITE UNIT

Petrology

Due to pervasive serpentinization, most samples do not contain primary magmatic minerals (Fig. 3.7.12(A) and (B)). However, in some samples, primary magmatic minerals are preserved. The main cumulus phases are olivine (typically 0.5–2 mm in width) and chromite (typically 0.1 mm).

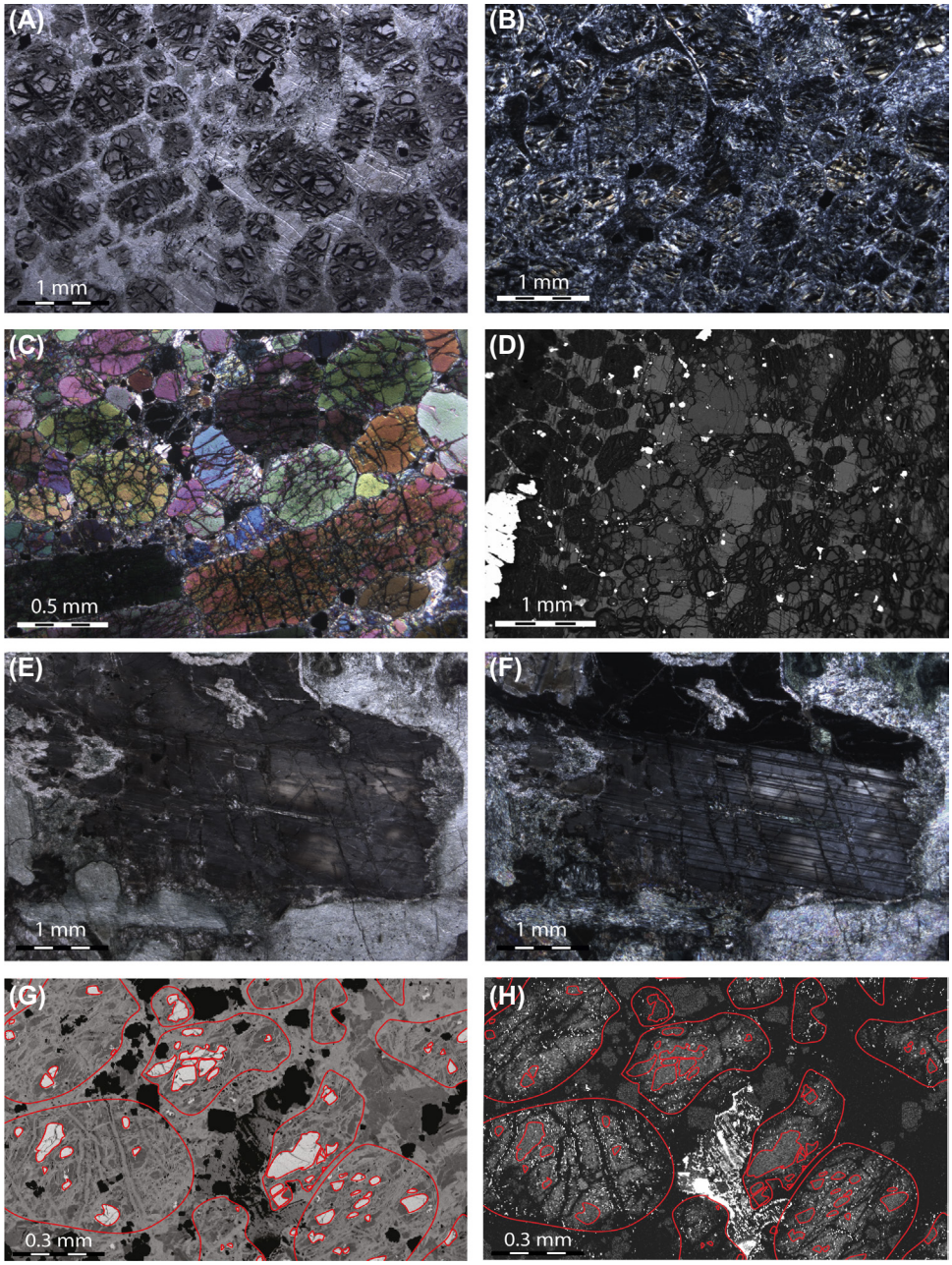

FIGURE 3.7.12 Images of thin sections from the peridotite unit.

(A) Serpentinized orthocumulate from the Sakatti main body, plane-polarized light; (B) serpentinized mesocumulate, crossed polarizers; (C) weakly altered olivine adcumulate from the dunite subunit, crossed polarizers; (D) backscattered electron image showing pargasite, enstatite, and diopside intercumulus and partially serpentinized olivine cumulate; (E) black plagioclase from the pegmatoidal gabbro subunit, plane polarized light; (F) black plagioclase from the pegmatoidal gabbro subunit, crossed polarizers; (G) wavelength-dispersive spectroscopy (WDS) chemistry map showing relative MgO contents of partially serpentinized olivine cumulate; cumulus olivine shapes have been outlined as well as their contained preserved olivine; (H) WDS chemistry map showing relative NiO contents of Fig. 3.7.12(G) showing variable Ni in preserved olivine as well as immobility of Ni during serpentinization.

Clinopyroxene is the most common intercumulus mineral, occurring as oikocrysts up to 2 cm across that are frequently altered to tremolite. Orthopyroxene also forms oikocrysts, but is less abundant.

The rock varies from orthocumulate to adcumulate on the 10^{-2} to 10^{2} m scale. Orthocumulate is more abundant toward the top of the succession, although there is local variability throughout. The dunite subunit is an adcumulate situated at the base of the intrusion. Rather than being distinct on a textural or primary mineralogical basis, it is different from the rest of the cumulate primarily because of an almost complete preservation of magmatic olivine (Fig. 3.7.12(C)). Possibly, the lack of intercumulus melt during crystallization has limited later serpentinization.

There are multiple occurrences within the peridotite package where olivine cumulate is absent and the rock is a coarse pyroxenite. These drill core intersections are generally less than 15 cm wide and are composed of up to 3-cm-sized diopside grains, as well as minor enstatite. These intersections could represent stratigraphically important levels, such as the tops of separate pulses of magmatism; however, to date, they do not correlate with the identified whole rock and mineral chemistry changes presented later in this section.

Pegmatoidal gabbro is similar to pyroxenite in that it contains very coarse pyroxene; pyroxenite could simply be a less evolved form of this subunit. The pegmatoidal gabbro is particularly prevalent in the central and eastern portions of the main cumulate body, and also toward its top. The down-hole thickness of the gabbroic intervals varies from less than 0.5 m up to 15 m, although the angle between the contacts and the core axis is highly variable and thus the true thickness remains unclear.

The pegmatoidal gabbro contains large euhedral plagioclase grains in addition to pyroxene and, possibly secondary, amphibole. Unusually, the plagioclase is black in color while the pyroxene is lighter gray. The rocks have sharp contacts to the surrounding cumulate and are frequently associated with mineralization (see Fig. 3.7.9(H)), either in the form of interstitial sulfides within the gabbro or as massive sulfides adjacent to the gabbro. It has not been possible to connect the coarse grained pyroxenites or the pegmatoidal gabbros laterally between boreholes, and their stratigraphic position does not appear to define chemical reversals. They are thus interpreted as late-stage dikes of more evolved melt, coeval with late-stage mineralization processes.

Mineral compositions

The composition of the main minerals was determined by electron microprobe at the Natural History Museum, London, using a Cameca SX 100 instrument.

Olivine

The olivine in the peridotites is characterized by Mg# (Mg# = atomic Mg/(Mg + Fe)) between 0.85–0.91 and Ni contents clustering between 3000–3500 ppm (Fig. 3.7.13). Compared to olivine from most other mafic–ultramafic intrusions with comparable Mg#, the Ni contents are relatively high, inconsistent with crystallization from a melt that was S saturated (Brenan and Caciagli, 2000).

In general, the Ni content of olivine does not vary significantly within the intrusion. However, some samples contain highly variable olivine Ni compositions, including a number of grains with a relatively low Ni content, similar to that of olivine in the aphanitic unit (Fig. 3.7.13). These crystals are relatively small in size (<20 μm) and are interpreted as entrained olivines derived from the footwall rocks.

In samples with significant disseminated mineralization, olivine may be zoned with decreasing Ni content toward grain margins (see Fig. 3.7.12(H)), possibly due to diffusive loss of Ni from olivine to surrounding sulfides or Ni-depleted silicate melt. However, zoning as a result of olivine growth in progressively Ni-depleted melt cannot be ruled out. Notably, Ni appears to be immobile during pervasive serpentinization. This is evident in an Ni distribution map of peridotite (see Fig. 3.7.12(H)), showing similar Ni contents in preserved olivine and serpentine.

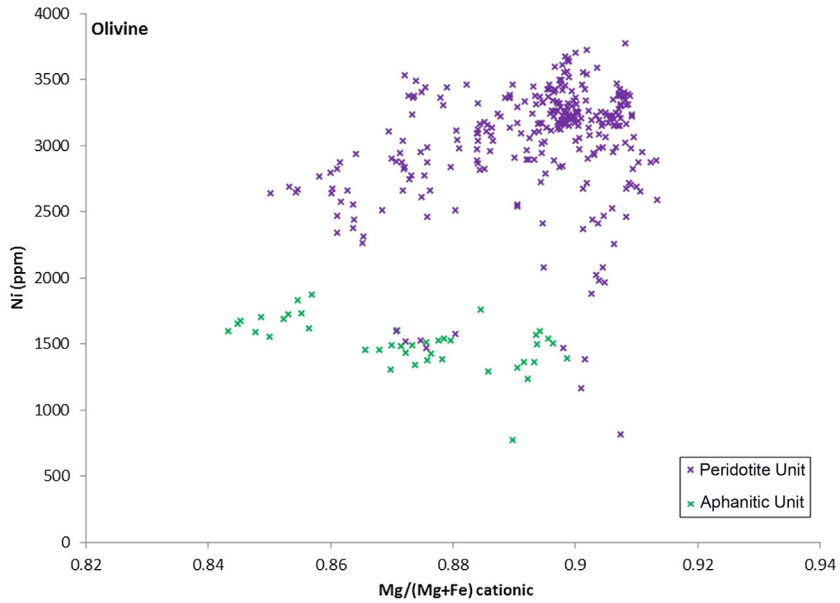

FIGURE 3.7.13 Olivine chemistry from the main cumulate body in the Sakatti deposit and the aphanitic footwall.

WDS (Wavelength Dispersive Spectra) data acquired on a Cameca SX100 EMPA (Electron Probe Micro Analyzer) at the Natural History Museum, London.

Overall, the olivine compositions are broadly comparable with "main ore" olivine chemistry reported from the Kevitsa deposit (Mutanen, 1997). At Sakatti, however, no olivine has been identified that approaches the unusual ultranickeliferous (up to 14,000 ppm) composition found in the "Ni-PGE ore" at Kevitsa (Yang et al., 2013).

Pyroxene

Pyroxene in the peridotite unit is invariably oikocrystic, surrounding and encompassing smaller cumulus olivine. Oikocrysts may be 1–2 cm wide. The pyroxene is frequently altered to tremolite-actinolite. In some cases, unaltered oikocrysts contain preserved olivine whereas surrounding olivine has been serpentinized. Enstatite oikocrysts have Mg# of 0.80–0.90 and Ni contents in the range of 400–1000 ppm, whereas diopside oikocrysts have Mg# of 0.85–0.92 and Ni contents of 200–600 ppm. Nickel contents correlate positively between ortho- and clinopyroxene in the same sample, but neither correlate with olivine Ni contents.

Amphibole

Chemical analyses reveal two distinct populations of amphibole. Amphiboles of the tremolite-actinolite series are the predominant type and are texturally identifiable as alteration products of pyroxene. In addition, there is a significant population of pargasite that is interpreted as a primary magmatic phase, based largely on texture (see Fig. 3.7.12(D)).

The presence of a magmatic hydrous phase has important implications for the composition of the melt (e.g., Fiorentini et al., 2008) and also raises the possibility of autoserpentinization associated with late-stage magmatic processes.

Plagioclase

Plagioclase is rarely present in the peridotite unit, except as an intercumulus phase near the contact with the aphanitic unit. This is interpreted to be a result of assimilation of rocks of the aphanitic unit, given the nature of the contact between the two units (see "Aphanitic Unit" section below). Plagioclase is also present in the pegmatoidal gabbroic rocks where it is black in hand specimens (see Fig. 3.7.12(E) and (F)). In both cases, the plagioclase is anorthite, although the Na:Ca ratio is variable.

Chromite

Chromite grains are euhedral and form the only other cumulus phase besides olivine. Most cumulus chromite has been altered to chrome-bearing magnetite. However, the grains frequently contain cores of chromite that potentially reflect the original composition. These cores have Cr_2O_3 contents between 27–37 wt% and Ni contents of 1000–2500 ppm. The presence of cumulus chromite suggests that the parental melt had an MgO content below 24 wt%, as otherwise chromite would not have been on the liquidus (Barnes, 1998). See details in Table 3.7.1.

Whole-rock chemistry

The whole-rock geochemical data for the majority of samples from the peridotite unit at Sakatti indicate primary control by accumulation of cumulus olivine (Fig. 3.7.14).

The MgO content of the parental melt from which the peridotite had formed can be estimated at approximately 19% using whole rock MgO and FeO contents, as well as olivine compositions (Bickle, 1982; Nisbet et al., 1993; Arndt, 2008; Fig. 3.7.15). Note that this estimate relies on a number of assumptions and should be treated with some caution (Arndt, 2008).

Identifying layering or separating different pulses of magmatism within the deposit has not been conclusive from simple drill core observations as the cumulate rocks are texturally relatively homogenous. Whole-rock chemical data have been used to delineate distinct pulses within the cumulate body (Fig. 3.7.16). The ratio (Mg + Fe)/Si is essentially controlled by modal proportions of olivine to pyroxene. In each drill core for which whole-rock geochemistry data are available it is possible to identify at least three separate magma pulses (Table 3.7.2).

Mineral chemistry data broadly confirm the separate layers seen in the whole-rock geochemistry, although sampling density is suboptimal due to the fact that most samples are pervasively serpentinized and therefore do not contain preserved magmatic minerals.

Trace element ratios are relatively uniform throughout the main cumulate body, both laterally and vertically, but tend to show some variations consistent with a relatively more contaminated signature (i.e., lower Nb-La, Nb/Th, and higher La-Sm, Th-Yb) in the upper part of the body (Fig.3.7.20).

The heavy rare earth elements (HREE) are relatively unfractionated, as indicated by primitive mantle-normalized Gd/Yb around 1.5. This suggests that garnet was not a residual phase during mantle melting, consistent with magma generation at relatively shallow depths of <90 km. Moderate crustal contamination of the mantle-derived melt prior to its emplacement is suggested by a number of trace element ratios (all normalized to primitive mantle values of McDonough and Sun, 1995), including Nb-La (0.15–0.45), Nb-Th (0.10–0.25), La-Sm (1.6–3), and Th-Yb (5–8).

Due to the moderately to highly incompatible nature of the lithophile trace elements, the information provided by these elements reflects primarily the composition of the intercumulus melt and may not necessarily be representative of the melt from which the cumulus phases (e.g., olivine) and sulfide mineralization formed (see "Mineralization" section below).

Table 3.7.1 WDS data showing representative mineral compositions of the main magmatic phases and their common alteration products in the main Sakatti cumulate body

	Olivine	Serpentine	Diopside	Tremolite	Enstatite	Pargasite	Plagioclase	Chromite	Magnetite
Na_2O	<0.05	<0.05	0.35	0.34	<0.05	2.37	2.26	na	na
MgO	48.73	36.06	17.47	19	31.88	19.02	0.05	5.52	1.45
Al_2O_3	<0.04	0.22	3.52	2.2	1.43	10.46	32.85	12.96	1.29
SiO_2	40.34	40.56	51.87	51.47	56.37	46.56	47.8	<0.03	<0.03
K_2O	<0.05	<0.05	<0.05	<0.05	<0.05	0.57	0.07	na	na
CaO	0.03	0.11	20.83	20.54	2.26	11.65	16.33	<0.02	<0.02
TiO_2	0.04	0.03	0.5	0.24	0.14	1.18	<0.02	0.35	0.43
Cr_2O_3	<0.04	<0.04	1.04	1.26	0.54	1.81	<0.04	33.04	11.63
V_2O_3	<0.04	<0.04	<0.04	<0.04	<0.04	0.06	<0.04	0.14	0.17
MnO	0.13	0.27	0.13	0.11	0.17	0.03	<0.03	0.61	0.23
FeO	10.22	8.4	4.36	3.5	7.51	4.61	0.51	43.6	78.82
CoO	<0.06	<0.06	<0.06	<0.06	<0.06	<0.06	<0.06	<0.06	<0.06
NiO	0.42	0.44	0.06	0.13	0.12	0.09	<0.02	0.07	0.14
Totals	100	86.12	100.2	98.82	100.5	98.41	99.87	96.34	94.19

na = not analyzed

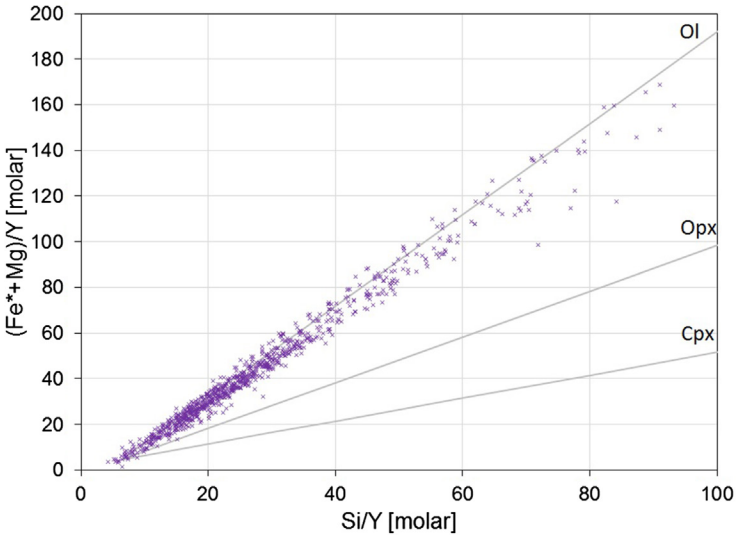

FIGURE 3.7.14 Whole-rock geochemistry plot showing Fe* + Mg versus Si normalized to Y for the peridotite unit in molar proportions.

Olivine (Ol), orthopyroxene (Opx), and clinopyroxene (Cpx) lines are calculated using WDS mineral data. All data recalculated volatile free; Fe* = Fe corrected to remove sulfide Fe.

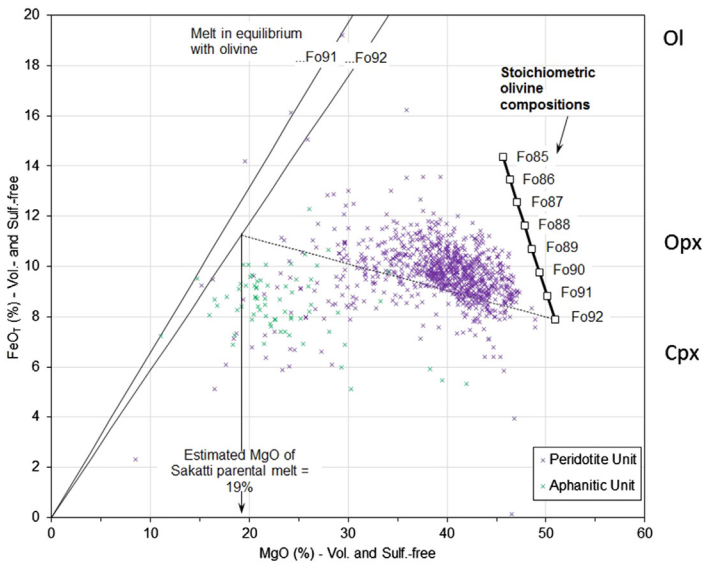

FIGURE 3.7.15 Binary variation plot of whole rock FeO_T versus MgO in peridotite and aphanitic units.

Data have been normalized to volatile and sulfide-free compositions. Melt-olivine equilibrium lines have been calculated assuming $KD_{(FeO/MgO_{Ol})/(FeO/MgO_L)} = 0.3$. *Arndt (2008).*

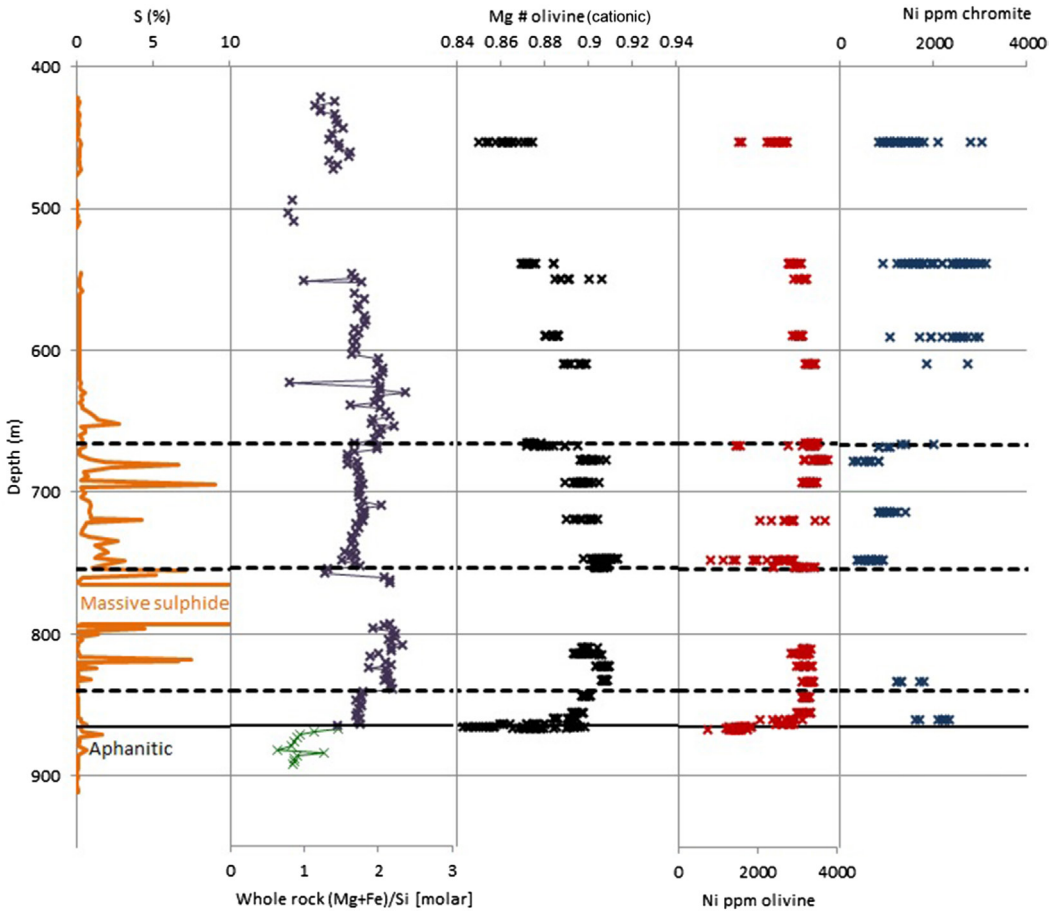

FIGURE 3.7.16 Down-hole plot showing whole-rock geochemistry and mineral chemistry data.

Plotted from left to right are: whole-rock S%, whole-rock (Mg + Fe/Si (volatile and sulfide corrected), WDS data for Mg/(Mg + Fe) in olivine, Ni ppm in olivine, and Ni ppm in chromite. Layers can be identified in the whole-rock geochemistry and these correlate broadly with subtle changes in mineral chemistry.

APHANITIC UNIT

Petrology

The unit is composed of a groundmass of fine-grained (20–50 μm) interlocking plagioclase and pyroxene in roughly equivalent proportions (~35–45% of groundmass each) and a smaller amount of fine-grained olivine (~15–20% of groundmass).

Phenocrysts of olivine and rare plagioclase make up about 10% of the rock, although the olivine phenocrysts are generally less than 1 mm in size and difficult to see in hand specimens. Olivine phenocrysts form elongate, narrow grains, with the longest one observed being a 4 mm × 0.2 mm single crystal (Fig. 3.7.17(A) and (C)). The cores of phenocrysts are frequently hollow. These are interpreted as extrusive olivine textures, which are compatible with the fine-grained nature of the groundmass. The

Table 3.7.2 Whole-rock geochemistry for major units of the Sakatti deposit

		Peridotite										
SiO_2	%	46.96	43.85	41.8	43.42	39.79	47.42	43.25	40.48	42.59	43.52	40.91
TiO_2	%	0.22	0.19	0.25	0.17	0.08	0.36	0.15	0.14	0.18	0.33	0.2
Al_2O_3	%	4.39	2.21	3.15	2.2	1.16	4.57	2.05	1.66	2.56	2.54	2.42
Fe_2O_3	%	1.61	1.59	1.69	1.45	1.32	1.4	1.54	1.32	1.48	1.6	1.76
FeO	%	9.67	9.54	10.15	8.72	7.94	8.39	9.24	7.91	8.88	9.59	10.54
MnO	%	0.11	0.16	0.17	0.18	0.18	0.22	0.14	0.13	0.18	0.16	0.13
MgO	%	29.21	39.76	37.88	41.53	46.12	30.74	40.09	46.26	41.55	38.74	40.5
CaO	%	6.48	0.9	1.98	0.76	1.48	5.22	1.03	0.57	0.8	1.61	1.21
Na_2O	%	0.11	0.07	0.24	<0.01	<0.01	0.49	<0.01	<0.01	<0.01	0.05	<0.01
K_2O	%	0.02	0.09	0.21	0.05	0.01	0.21	<0.01	0.04	0.12	0.08	<0.01
P_2O_5	%	<0.01	0.01	0.05	0.01	0.04	0.03	<0.01	0.02	0.04	0.05	0.03
LOI	%	8.5	13.1	11.9	14.8	15	9.3	14.4	15.3	14.1	12.1	13.4
C	%	0.26	0.13	0.15	0.13	0.55	0.11	0.21	0.13	0.18	0.1	0.24
S	%	0.5	0.2	0.9	0.43	0.13	0.23	0.66	0.11	0.14	0.53	1.23
Se	ppm	2.1	1.1	5.5	0.5	0.6	0.4	2.3	0.1	0.7	3.9	9.6
Ni	ppm	2645	2843	2625	2745	3077	1544	2914	2786	2497	2588	2574
Cu	ppm	172	376	5337	30	94	58	303	10	18	2021	7265
Co	ppm	109.2	130.7	131.3	125.1	131.5	93.7	133.7	117.4	131.2	111	182.5
Cr	ppm	3808	7469	7317	6212	9348	3738	11826	7023	8139	6228	3906
V	ppm	102	66	78	57	37	128	39	51	75	85	87
Sc	ppm	22	9	12	10	6	21	8	10	12	13	10
Zn	ppm	9.1	24.5	34.3	37.1	8.7	83.7	22.9	6.3	31.4	31.9	45.9
Rb	ppm	0.7	4	6.3	2.5	1.2	5.5	1.1	1.8	4.7	2.9	1.2
Sr	ppm	11.5	7.4	13.8	5.9	7.4	47.6	3.8	4.5	8	7.3	5
Ba	ppm	7	42	74	6	33	359	2	42	87	8	15

Th	ppm	0.3	0.5	0.6	0.5	<0.2	0.8	<0.2	0.2	0.2	0.6	0.2
U	ppm	<0.1	<0.1	0.1	0.1	<0.1	0.2	<0.1	<0.1	<0.1	<0.1	<0.1
Nb	ppm	0.4	0.1	<0.1	0.6	<0.1	0.9	<0.1	<0.1	0.4	1.6	0.7
Zr	ppm	12	13.6	22.9	12.1	5.5	22.6	15.6	10.4	18.3	30.9	14.8
Hf	ppm	0.4	0.5	0.6	0.2	0.2	0.8	0.4	0.2	0.5	0.8	0.3
Y	ppm	4	2.2	3.9	2.4	0.8	5.1	1.4	1.4	3.2	4.2	3.3
La	ppm	1.5	1.3	2.4	1	0.7	2.2	0.4	0.7	1.2	1.1	1.7
Ce	ppm	2.5	3.4	5	1.9	1.2	6.3	0.7	1.7	3.1	2.9	3.5
Pr	ppm	0.28	0.39	0.67	0.31	0.14	0.75	0.11	0.23	0.4	0.48	0.5
Nd	ppm	1.7	2.2	1.7	1.4	1.1	3.5	0.6	1.2	1.8	2.2	2.3
Sm	ppm	0.42	0.47	0.81	0.29	0.14	0.8	0.17	0.37	0.27	0.63	0.5
Eu	ppm	0.12	0.13	0.18	0.12	0.05	0.3	0.05	0.11	0.13	0.16	0.13
Gd	ppm	0.75	0.44	0.66	0.48	0.24	1.06	0.27	0.38	0.6	0.76	0.71
Tb	ppm	0.12	0.08	0.12	0.07	0.04	0.18	0.05	0.07	0.08	0.14	0.12
Dy	ppm	0.63	0.48	0.77	0.44	0.18	1.11	0.27	0.32	0.63	0.76	0.57
Ho	ppm	0.14	0.09	0.12	0.08	0.04	0.26	0.06	0.06	0.14	0.15	0.14
Er	ppm	0.42	0.27	0.41	0.32	0.08	0.7	0.17	0.18	0.27	0.42	0.34
Tm	ppm	0.06	0.04	0.06	0.04	0.02	0.08	0.02	0.02	0.05	0.07	0.05
Yb	ppm	0.42	0.26	0.31	0.29	0.11	0.6	0.19	0.2	0.29	0.37	0.4
Lu	ppm	0.06	0.06	0.06	0.04	0.01	0.09	0.02	0.04	0.04	0.06	0.06

Continued

Table 3.7.2 Whole-rock geochemistry for major units of the Sakatti deposit—cont'd

		Dunite (logging unit)		Altered Ultramafic			Aphanitic	
SiO_2	%	41.36	42.09	46.98	41.48	40.67	50.01	49.53
TiO_2	%	0.1	0.11	0.32	0.17	0.36	0.82	0.48
Al_2O_3	%	1.19	1.38	5.38	2.17	6.63	9.5	9.62
Fe_2O_3	%	1.4	1.5	1.42	1.27	0.9	1.34	1.37
FeO	%	8.39	8.98	8.52	7.6	5.37	8.02	8.21
MnO	%	0.13	0.14	0.18	0.14	0.09	0.13	0.14
MgO	%	44.51	42.92	29.53	37.85	26.62	20.7	20.51
CaO	%	0.79	0.95	6.35	7.9	16.84	6.65	7.39
Na_2O	%	0.07	0.05	0.18	0.04	1.59	2.25	2.08
K_2O	%	0.13	0.04	0.06	0.12	0.07	0.09	0.18
P_2O_5	%	0.02	<0.01	0.01	0.01	0.25	0.02	0.02
LOI	%	7.8	4.9	8.9	21.4	23.9	2.5	2.5
C	%	0.08	0.09	0.25	5.28	5.3	0.15	0.13
S	%	0.19	0.29	0.27	0.27	<0.02	0.06	0.12
Se	ppm	0.9	1.5	0.1	1.3	0.1	<0.1	0.2
Ni	ppm	3088	2795	1630	2990	1406	676	668
Cu	ppm	74	1443	85	923	41	41	47
Co	ppm	144.8	128.8	90.8	92.5	47	67.8	71.1
Cr	ppm	9478	7943	4739	4327	2643	1875	1947
V	ppm	54	41	120	71	112	188	140
Sc	ppm	6	7	18	10	13	29	32
Zn	ppm	18.7	19.4	27.6	3	6.5	11.8	17.9
Rb	ppm	5.9	2.8	2.2	5	3.7	2.4	4.8
Sr	ppm	3.6	8.8	16.8	36.6	83.3	96.7	91.8
Ba	ppm	13	21	18	4	46	74	62
Th	ppm	<0.2	<0.2	0.7	<0.2	2.2	0.9	0.4
U	ppm	<0.1	<0.1	0.2	<0.1	2.1	<0.1	<0.1
Nb	ppm	14.6	0.2	0.7	1.2	2.6	1.6	1.1
Zr	ppm	6.2	7	18.6	13.2	52.4	57.9	25.9

Hf	ppm	<0.1	0.2	0.6	0.4	1.5	1.6	0.9
Y	ppm	1.7	1.4	5.7	3.5	11.4	9.3	7.2
La	ppm	0.9	0.7	1.2	1.9	13.6	2.8	2.1
Ce	ppm	1.4	1.6	3.2	2.7	30.7	7	4.4
Pr	ppm	0.19	0.13	0.5	0.32	3.11	1	0.74
Nd	ppm	0.8	0.9	2.8	1.7	11.5	5.4	3.5
Sm	ppm	0.2	0.17	0.72	0.4	2.29	1.39	0.97
Eu	ppm	0.08	<0.02	0.21	0.05	0.6	0.38	0.34
Gd	ppm	0.24	0.2	1.01	0.54	2.08	1.79	1.32
Tb	ppm	0.06	<0.01	0.18	0.09	0.36	0.32	0.23
Dy	ppm	0.22	0.21	0.89	0.64	1.93	1.76	1.4
Ho	ppm	0.06	<0.02	0.22	0.15	0.49	0.38	0.27
Er	ppm	0.18	0.12	0.62	0.44	1.02	0.97	0.81
Tm	ppm	0.02	<0.01	0.08	0.05	0.16	0.13	0.13
Yb	ppm	0.13	0.11	0.57	0.38	1.2	0.91	0.8
Lu	ppm	0.02	<0.01	0.07	0.05	0.17	0.13	0.09

Note: FeO and Fe_2O_3 concentrations were calculated from Fe_2O_{3T} using a molar Fe_2O_3/FeO ratio of 0.15, typical of mantle-derived mafic–ultramafic magmas. All data are corrected to anhydrous compositions.

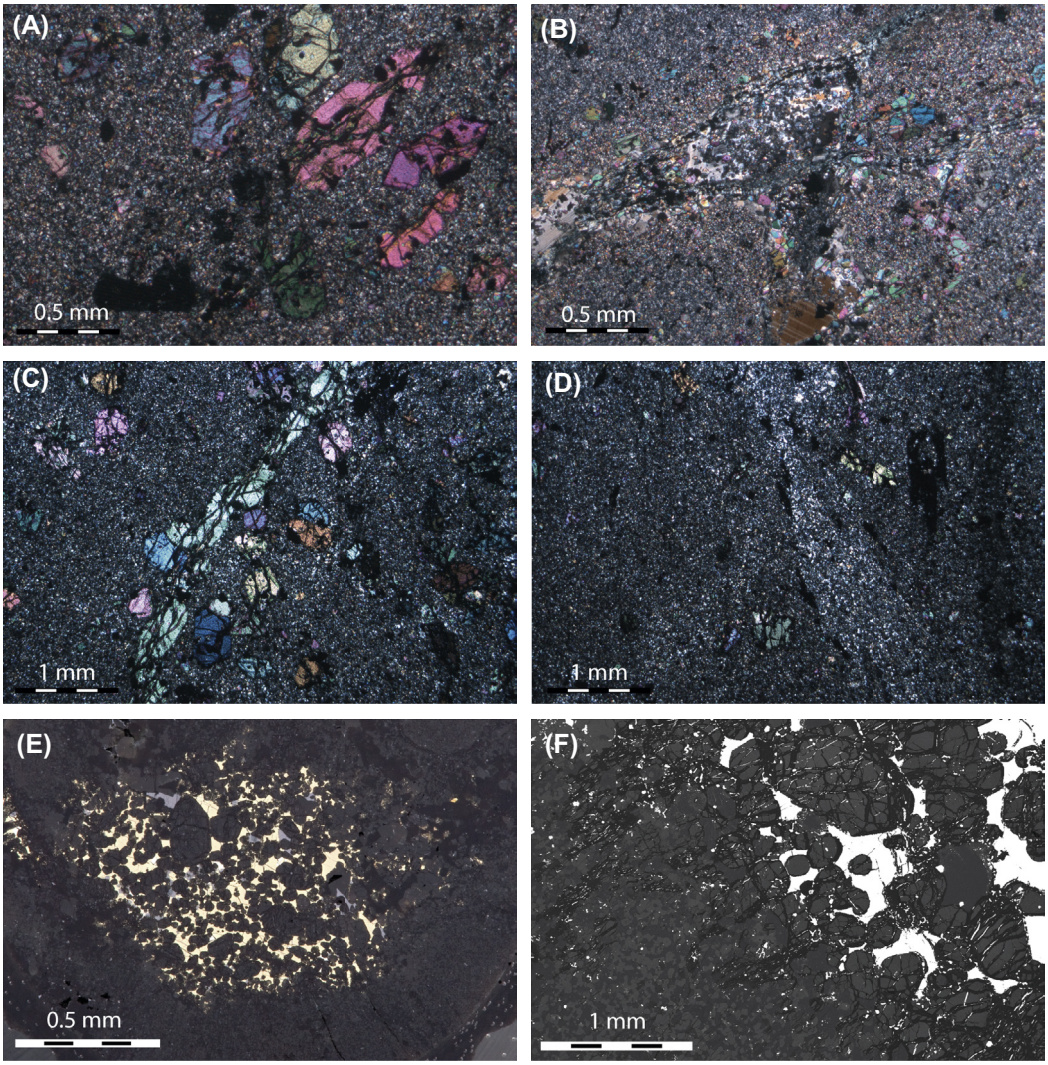

FIGURE 3.7.17 Images of thin sections from the aphanitic unit.

(A) Euhedral olivine in fine-grained pyroxene and plagioclase groundmass, typical of the aphanitic unit; (B) large plagioclase and olivine phenocrysts and serpentine veining; (C) elongate individual crystal of olivine and numerous smaller phenocrysts; (D) domaining of orthopyroxene- and clinopyroxene-dominated groundmass; (E) interstitial mineralization and olivine cumulate intruded into the aphanitic unit; (F) backscattered electron (BSE) image in Fig. 3.7.17(E) showing the difference between large cumulus olivines from the main cumulate body and phenocrystic olivine from the aphanitic unit.

chemistry of these olivines is similar to that of olivines in the peridotite unit, with Mg# of around 0.84–0.90. However, the Ni contents of the olivines in the aphanitic unit are distinctly lower (Ni 1800–1200 ppm) and do not exhibit the positive correlation with Mg# shown by the olivines of the peridotite unit (see Fig. 3.7.13).

Table 3.7.3 EDS (Energy Dispersive Spectra) data showing representative major element chemical composition of mineral phases in the Aphanitic Unit and their approximate proportions.

	Olivine (phenocryst)	Plagioclase (phenocryst)	Enstatite	Diopside	Olivine	Plagioclase	Ilmenite
Proportion of each	0.15	0.05	0.15	0.2	0.15	0.29	0.01
NaO	nd	5.4	nd	0.7	nd	7.3	nd
MgO	42.2	nd	31	16	42.9	nd	3.6
Al_2O_3	nd	27.6	0.7	2.1	nd	25.5	nd
SiO_2	39.4	54.7	56.9	52.8	40	59.2	nd
CaO	nd	10.8	1.2	21.5	nd	7.7	nd
TiO_2	nd	nd	nd	0.8	nd	nd	52.9
Cr_2O_3	nd	nd	nd	0.7	nd	nd	nd
MnO	nd	nd	nd	nd	nd	nd	0.6
FeO	18.5	0.7	11.8	5.4	17.2	0.5	42.9
Total	100.1	99.2	101.6	100	100.2	100.3	100.1

nd = not detected
Source: *Data acquired on the Zeiss EVO 15 LS at the Natural History Museum, London.*

Plagioclase is present as small crystals in the groundmass and as larger crystals (up to 3 mm in length) containing numerous inclusions of olivine but not pyroxene (Fig. 3.7.17(B)). These larger crystals were originally thought to be of hydrothermal origin; however, analysis revealed them to be more Ca-rich than their groundmass equivalents (Table 3.7.3). Thus, these plagioclase grains are interpreted as phenocrysts. Pyroxene is present only as a groundmass phase. As in the peridotite unit, orthopyroxene and clinopyroxene are present as enstatite and diopside respectively. These two pyroxenes are present in distinct domains, so that part of a sample is enstatite-dominated, whereas other parts are dominated by diopside (see Fig. 3.7.12(D)).

Texturally, the rock exhibits considerable variability and domaining of minerals at the microscopic and hand specimen scale, which is interpreted as autobrecciation. Unaltered samples of this rock appear relatively homogenous, with minor serpentine veining being the only discernible texture. However, in more altered samples, separate domains become more obvious. Finer, moderately brecciated domains alternate with coarser, more homogenous layers. These are interpreted as flow-tops and cumulate portions, respectively. The relatively thin cumulate portions (<20 m) are distinct from the peridotites of the main cumulate body in that the former are finer-grained, much less serpentinized, and have exclusively orthocumulate textures.

Alteration

One of the most striking characteristics of the aphanitic unit is that it is, in general, remarkably unaltered and composed almost entirely of fine-grained primary magmatic minerals. Small black serpentine veinlets are concentrated around lineations of phenocrysts, and the long axes of olivine crystals appear to be particularly susceptible.

In some occurrences, the aphanitic unit can be more pervasively altered. This does not appear to be spatially related to the peridotite unit. Instead, strongly altered segments can occur sporadically within the aphanitic unit, but particularly so in the vicinity of its contact with the hanging wall lithologies.

Whole-rock chemistry

As this unit is relatively unaltered, the whole-rock chemistry is particularly reliable in reflecting the original magmatic composition (see Table 3.7.2). The MgO contents of the rocks typically range between 19 and 22 wt% but may reach up to 30 wt%.

Such a high MgO content could, at first, appear to be in disagreement with petrological results, which show the unit to contain up to 35% plagioclase. However, the mineral chemistry (see Table 3.7.3) and the approximate proportions of each mineral from petrological observations were found to be in good agreement with the whole-rock geochemistry. The typical Na content of 1.5–2.5 wt% in the whole rock is reflective of the plagioclase content and is not related to alteration.

The observed variations in whole-rock major element geochemistry within the aphanitic unit are not consistent with simple addition and subtraction of olivine, but rather suggest the presence of plagioclase and olivine phenocrysts (Figs. 3.7.18 and 3.7.19).

Classification of the aphanitic unit

The rocks cannot be readily defined as ultramafic because they contain more than 10% felsic minerals; nor can they be defined as ultrabasic because they have more than 45 wt% SiO_2 (Le Maitre et al., 2002). High MgO content of more than 18 wt% precludes classification as a basalt. The lack of alteration and the high plagioclase content suggest that the Na values reflect the original magmatic values.

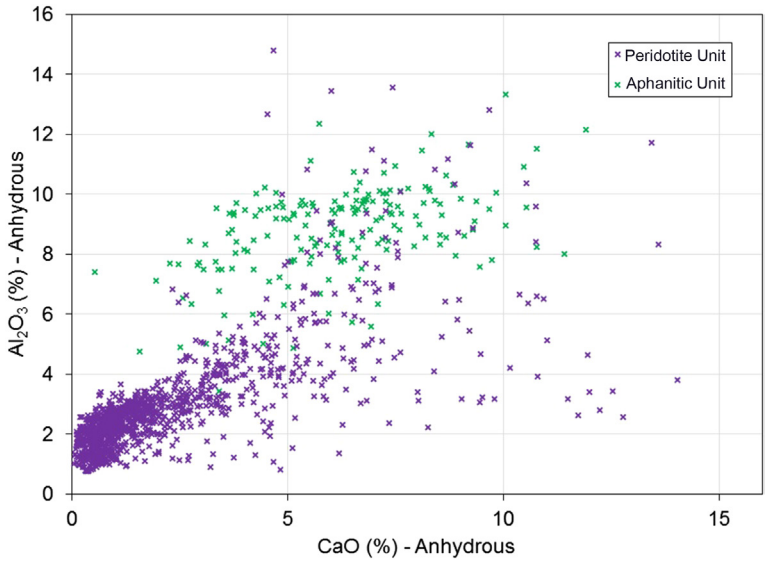

FIGURE 3.7.18 Binary variation diagram of whole-rock CaO versus Al_2O_3 for the peridotite and the aphanitic units.

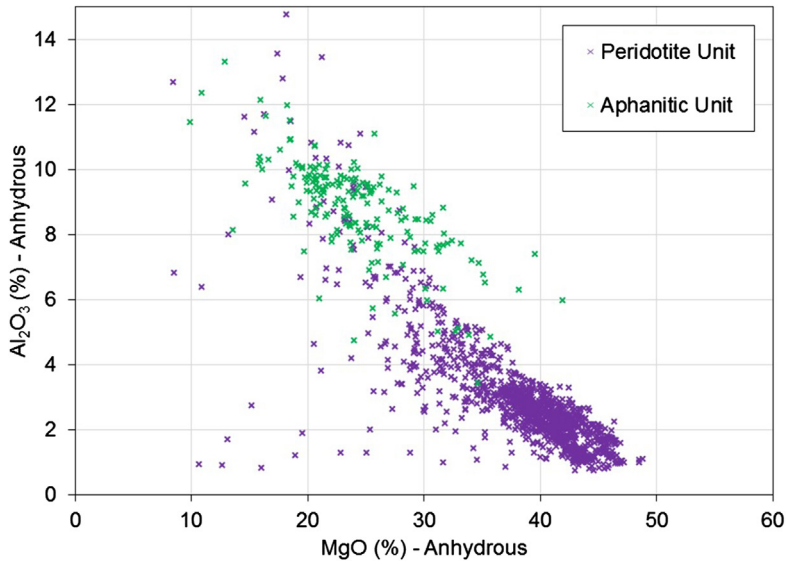

FIGURE 3.7.19 Binary variation diagram of whole-rock MgO versus Al_2O_3 showing both the peridotite and the aphanitic units.

The trend in the peridotite unit is consistent with olivine accumulation/dilution while the aphanitic unit shows a higher Al trend. This is potentially due to the presence of both olivine and plagioclase phenocrysts together.

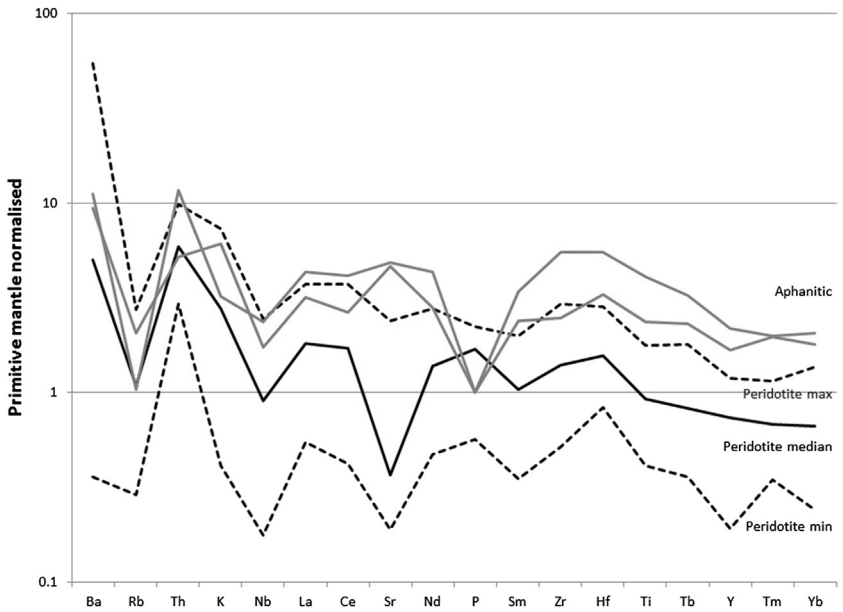

FIGURE 3.7.20 Trace element concentrations in representative samples of the peridotite and the aphanitic units.

Elements are arranged in order of compatibility and normalized to primitive mantle. *Normalization factors from McDonough and Sun (1995).*

According to Arndt (2008), the term komatiite should "be reserved solely for lavas with characteristic spinifex-textured olivines, or lavas that can be related directly, using field or petrological criteria, to lavas of this texture." Olivine spinifex texture is clearly identifiable in a 2-m section of one drill hole at the contact between the aphanitic unit and the peridotite unit. However, at present this is the only documented occurrence of olivine spinifex texture that has been observed in 155 drill holes and 99,388 m of diamond drilling.

For the purposes of this chapter it is deemed that this single occurrence of spinifex, lacking clear field relationships, is an insufficient basis on which to classify this unit as komatiitic. Furthermore, the high plagioclase content of this rock, meaning it is mafic rather than ultramafic, would make it an atypical komatiite. It is therefore termed a "plagioclase-rich picrite" on the basis of its high MgO content (Fig. 3.7.21). However, it is acknowledged that with the discovery of more olivine spinifex textured rocks, with clear field relationships, this definition could well be revised to a komatiite.

Nature of the contact between the peridotite and the aphanitic units

The contact between the peridotite unit and the aphanitic unit is generally diffuse, with the peridotite cumulate rock becoming more plagioclase- and pyroxene-rich (up to 30% pyroxene and 5% plagioclase) over an interval of 20–50 m approaching the contact. Despite the differing intercumulus material, the rock still remains identifiable as a cumulate and the Ni content of olivine does not change.

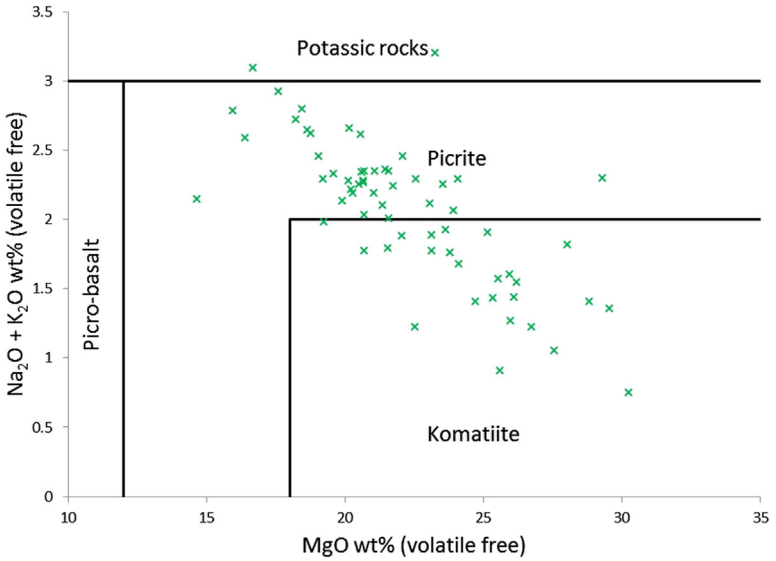

FIGURE 3.7.21 Whole-rock geochemistry of the aphanitic unit plotted according to the International Union of Geological Sciences (IUGS) komatiite-picrite definition.

All values are anhydrous.

Source: *From Le Maitre et al. (2002).*

In close proximity to the peridotite cumulate, the aphanitic unit contains 0.5–5 cm wide fingers or veinlets of peridotite. Within these fingers, cumulus euhedral olivine grains of up to 2 mm are distinguishable, identical to those in the peridotite unit (see Fig. 3.7.17(E) and (F)). In some cases, interstitial disseminated sulfide mineralization is present within the fingers (refer to Figs. 3.7.4(E) and 3.7.17(E) and (F)).

Microscopic analysis reveals that while the fingers are often relatively serpentinized, the surrounding aphanitic unit is usually relatively unaltered, retaining the fine-grained texture of plagioclase and pyroxene. Analysis of the mineral chemistry confirms the distinct nature of the two rock types as the olivine grains in the fingers exhibit a high Ni content while the olivines in the aphanitic unit have the low Ni content characteristic of this unit. It is also noted that generally the contacts between the fingers and the aphanitic unit are rich in large plagioclase crystals containing inclusions of olivine but no pyroxene. The origin of this texture is considered further in the "Discussion" section.

MINERALIZATION

Massive sulfides

The massive sulfides are characterized by a mixture of chalcopyrite and pyrrhotite-pentlandite (Fig. 3.7.22(A)). Pyrrhotite frequently carries up to 1 wt% Ni and contains small pentlandite "flames" orientated perpendicular to crystal boundaries (Fig. 3.7.22(G)). Pentlandite is often partly altered to violarite or less commonly millerite, particularly in samples where pyrite is present. Euhedral magnetite (typically 2–5 mm) is present throughout the massive sulfides and is interpreted to have crystallized from the sulfide liquid.

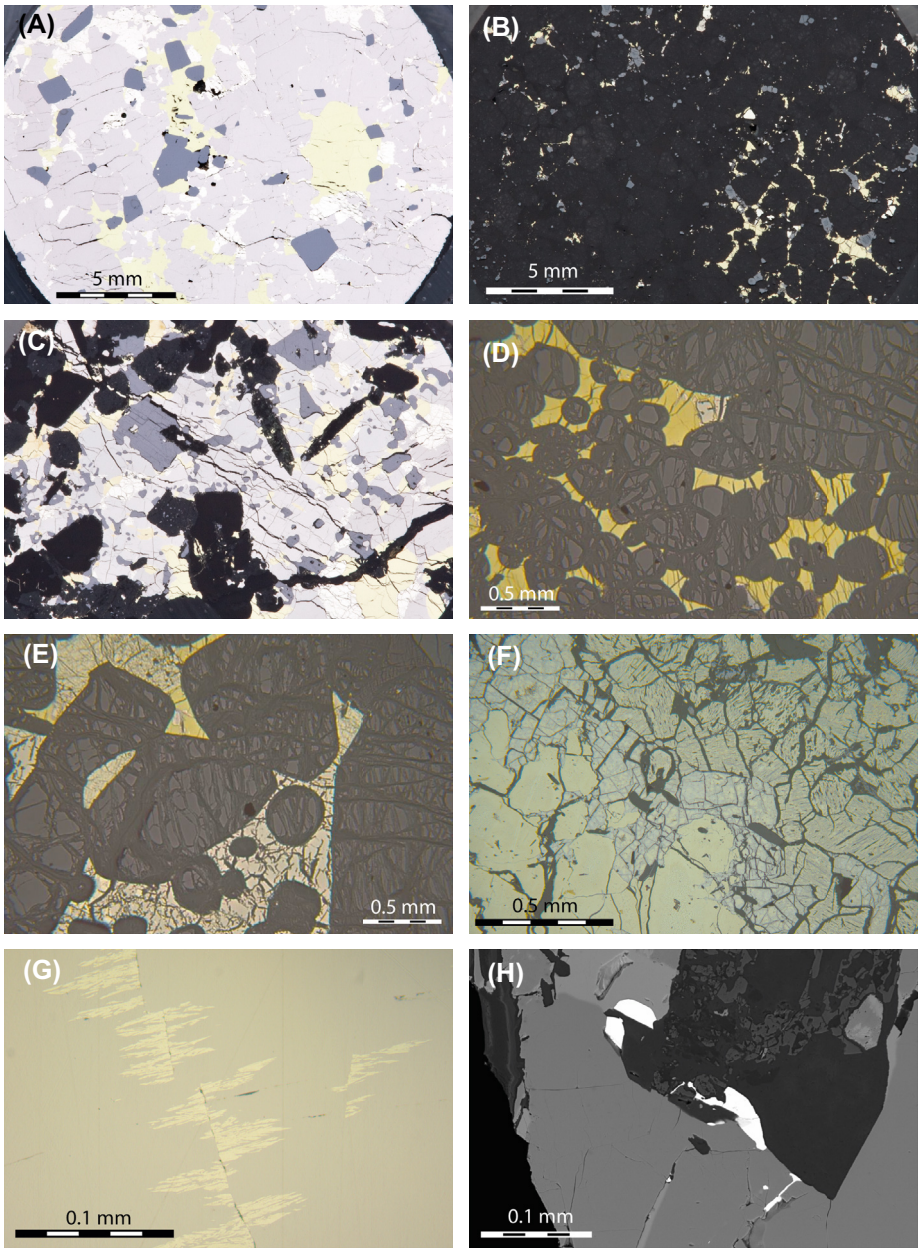

FIGURE 3.7.22 Polished block images of mineralization.

(A) Typical pyrrhotite-pentlandite massive sulfides with euhedral magnetite; (B) typical chalcopyrite-dominated disseminated sulfides in olivine cumulate; (C) semi-massive mineralization with large laths of black plagioclase and amphibole/pyroxene; (D) typical chalcopyrite-dominated disseminated mineralization interstitial to olivine cumulate; (E) atypical pyrrhotite-pentlandite disseminated mineralization in olivine cumulate; (F) pyrite-dominated mineralization containing (*left to right*) clean cobaltiferous pyrite, pentlandite, and violarite- and Ni-rich pyrite with magnetite lamellae; (G) pentlandite flames in pyrrhotite; (H) merenskyite (white) at a sulfide-silicate grain boundary.

PGE minerals of the merenskyite-moncheite-melonite series are present as small inclusions (1–100 μm), always associated with sulfide and primarily on grain boundaries of sulfide with either magnetite, silicate, or other sulfide (Fig. 3.7.22(H)). They have not been identified as being preferentially associated with any particular sulfide phase.

Pyrite is characteristic of the mineralization in the northeastern body, but it is also present in the main body, frequently toward the base of massive sulfide lenses. Pyrite is typically present as semi-spherical patches within other sulfides. This type of pyrite is frequently Co-rich (up to 1 wt.%) and Ni-poor. Where this pyrite is dominant, the interstitial spaces between the pyrite patches usually comprise Ni phases and Ni-rich pyrite with exsolved magnetite lamellae within it (Fig. 3.7.22(F)). The Ni phases comprise pentlandite, violarite, and minor millerite.

Vein sulfides

Sulfide veins are generally narrower than massive sulfide lenses and have variable orientations. The veins consist predominantly of chalcopyrite with minor pentlandite and pyrrhotite. Euhedral magnetite tends to be absent in this style of mineralization, distinguishing it from the massive sulfides. Platinum and Pd tenors are high and merenskyite-moncheite-melonite series tellurides are the only PGE minerals.

Disseminated sulfides

Disseminated sulfide mineralization occurs almost exclusively in the cumulate bodies, but can also be present in insignificant quantities in peridotite fingers within the aphanitic unit. Although the disseminated sulfides generally occur in the same portion of the cumulate body as the massive sulfides, they are not directly spatially related to the latter and are frequently more abundant distal from the massive sulfides. They are usually present as isolated, rounded blebs located interstitial to the olivines.

Chalcopyrite is invariably the dominant sulfide mineral in the disseminated mineralization. Magnetite lamellae are commonly present within chalcopyrite. The disseminated mineralization shares the same PGE mineralogy as the massive sulfides, with all PGE minerals being tellurides of the merenskyite-moncheite-melonite series.

Geochemistry

The distribution of Ni-Cu ratios within the deposit is not uniform. Massive sulfides show a shift in Ni-Cu ratios from relatively Ni-rich deep portions of the body in the northwest to relatively Cu-rich shallower portions in the southeast (Fig. 3.7.10). Vein and disseminated sulfides are generally more Cu-rich than massive sulfides. The Cu tenor of disseminated sulfides shifts from being relatively low in the northwest to relatively high in the southeast (Fig. 3.7.11). In the disseminated ore type, Pt and Pd occur roughly in the ratio of 2:1, which is not far from the average Pt-Pd ratio (1.8) measured for disseminated sulfides in the Kevitsa ore deposit (Mutanen, 1997). (See Table 3.7.4.)

The concentrations of the iridium-group PGEs (IPGE: Os, Ir, Ru) and palladium-group PGEs (PPGE: Rh, Pt, Pd) show variable primitive mantle-normalized patterns (Fig. 3.7.23) consistent with sulfide liquid fractionation in the massive sulfides (e.g., Ebel and Naldrett, 1996). Cu-rich sulfides are enriched in Pt and Pd and depleted in Os, Ir, Ru relative to Ni-rich sulfides. The disseminated sulfide samples show the same enrichment and depletion pattern as the Cu-rich massive sulfide (Fig. 3.7.23). Both the Ni-Cu and IPGE/PPGE ratios indicate that the Sakatti deposit has experienced considerable fractionation of the sulfide liquid.

Table 3.7.4 Whole-rock geochemistry showing examples of PGE, Ni, Cu, and Au values from mineralization in the Sakatti deposit

		Disseminated				Vein style			Massive (Cu-rich)				Massive (Ni-rich)			
Ni	%	0.22	0.04	0.20	0.20	0.05	0.5	1.21	0.6	1.93	1.70	4.22	4.9	4.76	8.16	9.46
Cu	%	3.22	0.6	0.20	0.26	0.05	6.95	18.44	28.4	6.55	2.60	5.84	2.24	1.92	2.23	2.34
S	%	3.78	1.59	0.43	1.87	0.10	10.13	28.55	30.84	16.68	43.46	32.26	34.02	33.51	35.16	23.69
Os	ppb	3	2	2	2	2	0.5	2	1	0.5	23	9	16	22	22	6
Ir	ppb	1	1	2	2	2	1	0.5	0.5	0.5	24	7	27	36	33	7
Ru	ppb	7	4	7	5	7	2	17	14	3	10	8	10	15	12	7
Rh	ppb	11	2	2	2	3	10	227	121	13	52	8	59	100	99	14
Pt	ppb	4941	2666	3136	2387	1124	15273	2443	1503	19618	2653	2469	1399	1935	472	1255
Pd	ppb	1644	1628	1307	1445	126	2064	26	1025	4010	1418	6095	1626	3536	1904	4198
Au	ppb	365	33	66	96	178	3119	2397	999	911	15	489	118	39	325	954

Note that grades across the deposit are variable, and while the reported values are typical, they are not meant to be representative of the whole deposit.

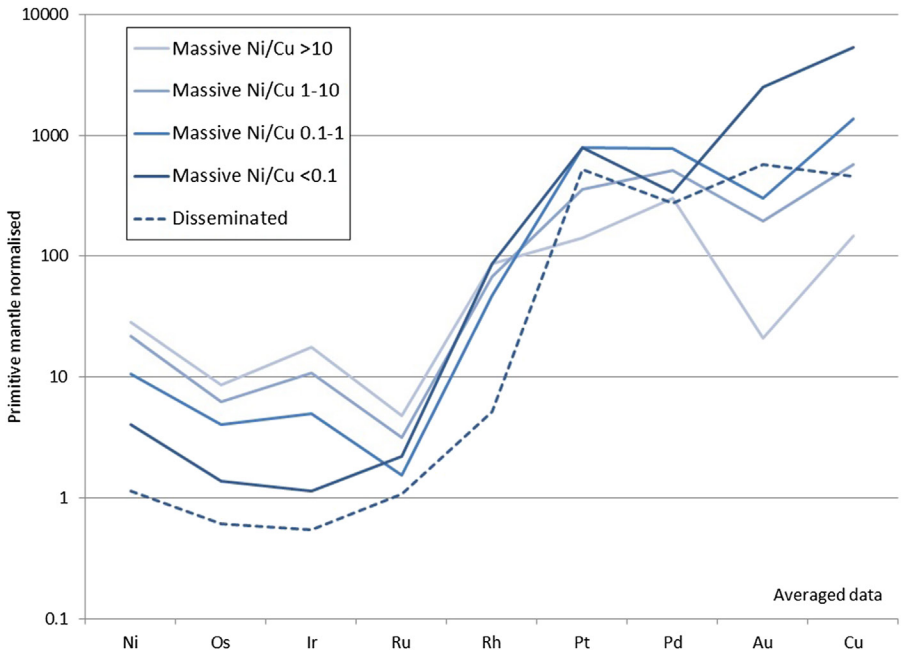

FIGURE 3.7.23 Whole-rock PGE, Ni, Cu, and Au data normalized to primitive mantle.

Massive sulfide data have been grouped according to Ni-Cu ratio. Vein sulfides have not been separated from massive sulfides. Note that the data are not normalized to 100% sulfide. *Normalization factors from McDonough and Sun (1995).*

S isotopes

The sulfides from the Sakatti deposit have a relatively uniform $\delta^{34}S$ (Vienna Canyon Diablo Troilite or VCDT) averaging +3‰ (Brownscombe et al., 2013). While sulfide-bearing sediments have not been intersected at Sakatti, samples of black schist from the Matarakoski formation in the surrounding area exhibit a wide spread of $\delta^{34}S$ (VCDT) signatures (Fig. 3.7.24). This is consistent with previous studies on the Matarakoski formation (Grinenko et al., 2003). The fact that the Sakatti data are so homogenous and plot relatively close to mantle values suggests that S saturation in the deposit is unlikely to have been caused by localized, in situ assimilation of the Matarakoski formation sediments.

Consistent with the S isotope results, S-Se ratios within the deposit (1500–4000, 10th to 90th percentile) are also in the range of typical mantle values, and likewise do not provide any evidence for assimilation of crustal S. The lower end of the range of S-Se ratios tends to be associated with Cu-rich sulfide, consistent with the experimentally derived partitioning behavior of S and Se in fractionating sulfide (Helmy et al., 2010).

If assimilation of S within the crust had occurred, the assimilant must have had $\delta^{34}S$ and S-Se signatures close to mantle values, and assimilation must have occurred prior to final emplacement allowing for high *R* factors and complete homogenization of the resultant disseminated and massive sulfides.

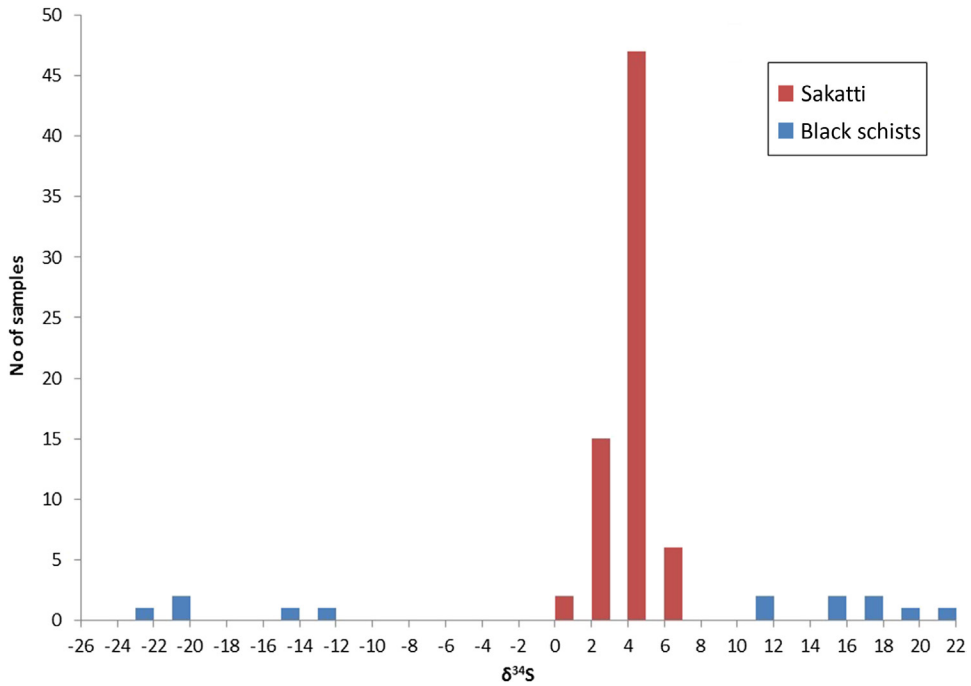

FIGURE 3.7.24 Histogram showing $\delta^{34}S$ values of sulfides from the Sakatti deposit and the regional Matarakoski formation black schists.

Analysis was undertaken at the Scottish Universities Environmental Research Centre, Glasgow.

Source: *From Brownscombe et al. (2013).*

Anhydrite is present within the intrusion, sometimes associated with pyrite. The pyrite has typical Sakatti $\delta^{34}S$ values of +3‰ whereas the anhydrite has $\delta^{34}S$ values of +10‰. Although it is theoretically possible that the anhydrite is externally derived, the fact that sulfides in close proximity do not show elevated $\delta^{34}S$ values is inconsistent with this hypothesis. Instead, the anhydrite is interpreted to be an oxidation product of magmatic sulfides.

Platinum-group element minerals

It is estimated that between 30 and 50% of the measured Pd in the massive sulfides resides in solid solution within pentlandite, based on LA-ICP-MS (Laser Ablation Inductively Coupled Plasma Mass Spectrometry) analysis and mass balance on eight samples from two drill holes. The remainder of the Pd and all of the Pt is located within telluride minerals of the moncheite-merenskyite-melonite series and minor michenerite. A wide range of Pt-Pd-Ni compositions is observed, which is unusual for this series (Fig. 3.7.25). By contrast, in the majority of known occurrences, these tellurides are restricted to either a Pt-Pd trend or a Pd-Ni trend (Helmy et al., 2007). Departure from these two trends, as well as the overall dominance of telluride phases, is shared by the Kevitsa deposits (Gervilla and Kojonen, 2002).

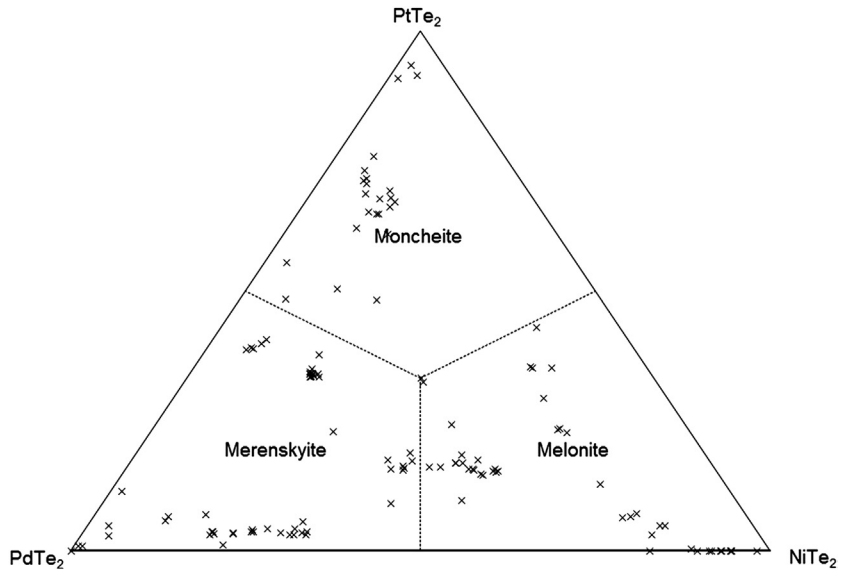

FIGURE 3.7.25 Chemistry of the PGE phases at the Sakatti deposit in atomic proportions.

Source: *Measured by WDS using the Cameca SX 100 at the Natural History Museum, London.*

DISCUSSION

INTRUSIVE VERSUS EXTRUSIVE

The Sakatti main cumulate body has been interpreted as a shallow level, conduit-like intrusion (Brownscombe et al., 2013) or as a cumulate portion of the picritic-komatiitic lava flows forming the aphanitic unit (T. Halkoaho, personal communication, 2014). While it is true that the Sakatti main cumulate body is hosted by volcanic rocks, and ultrabasic lava successions are known to have associated peridotitic to dunitic cumulate bodies, there are several lines of evidence that suggest that Sakatti is not a lava channel cumulate but an intrusion into a lava flow field:

- The tubular shape of the cumulate body (see Fig. 3.7.10).
- The peridotite has an apparent intrusive contact with the aphanitic unit both above and below the cumulate body, with finger-like intrusions of cumulate peridotite into the aphanitic footwall and hanging wall.
- The cumulate body is texturally and chemically different from the aphanitic unit such as the abundant plagioclase and low Ni contents of olivine in the latter. The aphanitic unit itself contains minor interlayered cumulate portions, that are distinct from the cumulate unit.
- The cumulate body is large and homogenous. It is more than 400-m thick in sections, with no clear evidence of flow tops or chilled margins.

It is suggested that the aphanitic unit and the main peridotite cumulate body are probably related to the same magmatic event and the same magmatic feeder system, but that the main cumulate body was formed slightly later as a subvolcanic intrusion.

NATURE OF CONTACT WITH THE APHANITIC UNIT

The contact between the peridotite unit and the aphanitic unit in both the hanging wall and the footwall consists of fingers of peridotite injecting into the lava.

This pattern of microintrusions suggests that the peridotite exploited a preexisting texture or weakness in the aphanitic unit. Petrographic examination of samples of the aphanitic unit reveal a network of fine serpentine veins that are concentrated along olivine and plagioclase phenocrysts.

It is proposed that the serpentine veining occurred prior to emplacement of the main cumulate body, or was potentially associated with it. The zones of hydrated microveins along with plagioclase phenocrysts would have a lower solidus than the rest of the aphanitic rock, resulting in preferential melting during emplacement of the peridotite and local injection of the latter.

DECOUPLING OF THE COMPOSITION OF OLIVINE AND SULFIDE MINERALIZATION

Olivine within the main cumulate body contains relatively high concentrations of Ni, which indicates crystallization from a melt that had not been depleted in Ni in response to segregating sulfide melt. Furthermore considering the primitive nature of the host rocks, the mineralization is, overall, unusually Cu-rich. These observations imply that the olivine was not in equilibrium with the sulfide melt. The current silicate host cannot, therefore, be considered as having crystallized from magma parental to the sulfides.

It is proposed that the sulfides were initially deposited by earlier magmatic activity "upstream" in the Sakatti conduit system and were subsequently remobilized by an olivine-charged silicate magma to be deposited in the current location. In addition, sulfide liquid was mobilized during or after in situ sulfide melt fractionation to form distinct veins of massive sulfides. The veins are relatively Cu rich because Cu-rich residual liquid has a lower solidus than the silicate melt. This model is consistent with the sharp contacts of the massive sulfide lenses and veins and their intrusion into the footwall where they continue to undergo fractionation.

SUMMARY

The Sakatti Cu-Ni-PGE deposit is a Cu-rich magmatic Ni sulphide deposit hosted by an olivine cumulate.

- The footwall and in some places hanging wall rock is a high Mg volcanic succession.
- The cumulus olivine contains high Ni values, up to 3700 ppm.
- Disseminated sulphide mineralisation is Cu-dominated and shows evolved PGE patterns.
- Massive sulphide mineralisation can be either Ni- or Cu-dominated, shows clear spatial zonation in Ni/Cu ratios, and indicates typical sulphide fractionation.

The deposit is interpreted as a conduit-like intrusion through the volcanic succession. Sulphide formation is inferred to have occurred at an earlier stage and undergone a degree of fractionation before being remobilised by the current silicate host.

ACKNOWLEDGMENTS

The Anglo American Finland Exploration team has been a tight-knit unit and has seen discovery of this deposit through to the current level of understanding. All of the work presented builds on the work of the team, which includes, but is not limited to, geologists Sebastian Stelter, Ryan Preece, Klara Collis, Peter Dodds, Louise Wright, and Catherine Reynolds.

Special thanks go to Brian Williams and Denis Fitzpatrick who were crucial in the discovery of Sakatti. In addition, Johanna Alitalo and Jorgen Ylitalo were part of the team during the discovery period, and deserve credit. Furthermore, without the belief and support of Owen Bavinton and Graham Brown, Sakatti would not have been discovered by Anglo American.

Thanks also go to the current Sakatti project manager Jukka Jokela and to Tapio Halkoaho (GTK) for stimulating discussions.

Anglo American is thanked for the permission to publish this chapter.

Thanks are due to Jamie Wilkinson of the Natural History Museum, London, who was a supervisor of the senior author's (W. Brownscombe) Ph.D. project from which this chapter arose. Thanks are also due to Anton Kearsley and John Spratt of the Natural History Museum, London, for their assistance with SEM and EPMA techniques.

REFERENCES

Arndt, N.T. (Ed.), 2008. Komatiite, second ed, Cambridge University Press, Cambridge, p. 467.

Barnes, S.J., 1998. Chromite in komatiites: 1. magmatic controls on crystallisation and composition. Journal of Petrology 39, 1689–1720.

Bickle, M.J., 1982. The magnesium contents of komatiitic liquids. In: Arndt, N.T., Nisbet, E.G. (Eds.), Komatiites. George Allen and Unwin, London, pp. 479–494.

Brownscombe, W., Herrington, R.J., Wilkinson, J.J., et al., 2013. Geochemistry of the Sakatti magmatic Cu-Ni-PGE deposit, northern Finland. In: Proceedings of the 12th Biennial SGA Meeting on Mineral Deposit Research for a High-Tech World, August 12–15, Uppsala. Geological Survey of Sweden, Uppsala, pp. 956–959.

Brenan, J.M., Caciagli, N.C., 2000. Fe-Ni exchange between olivine and sulphide liquid: implications for oxygen barometry in sulphide-saturated magmas. Geochimica et Cosmochimica Acta 64, 307–320.

Ebel, D.S., Naldrett, A.J., 1996. Fractional crystallization of sulfide ore liquids at high temperature. Economic Geology 91, 607–621.

Fiorentini, M.L., Beresford, S.W., Deloule, E., et al., 2008. The role of mantle-derived volatiles in the petrogenesis of Palaeoproterozoic ferropicrites in the Pechenga greenstone belt, northwestern Russia: Insights from in-situ microbeam and nanobeam analysis of hydromagmatic amphibole. Earth and Planetary Science Letters 268, 2–14.

Gervilla, F., Kojonen, K., 2002. The platinum-group minerals in the upper section of the Keivitsansarvi Ni-Cu-PGE deposit, northern Finland. Canadian Mineralogist 40, 377–394.

Grinenko, L.N., Hanski, E., Grinenko, V.A., 2003. Formation conditions of the Keivitsa Cu-Ni deposit, northern Finland: Evidence from S and C isotopes. Geochemistry International 41 (2), 154–167.

Hanski, E., Huhma, H., 2005. Central Lapland Greenstone Belt. In: Lehtinen, M., Nurmi, P.A., Rämö, O.T. (Eds.), The Precambrian Geology of Finland—Key to the Evolution of the Fennoscandian Shield. Elsevier, Amsterdam, pp. 139–193.

Helmy, H.M., Ballhaus, C., Berndt, J., et al., 2007. Formation of Pt, Pd and Ni tellurides: experiments in sulphide-telluride systems. Contributions to Mineralogy and Petrology 153, 577–591.

Helmy, H.M., Ballhaus, C., Wohlgemuth-Ueberwasser, C., et al., 2010. Partitioning of Se, As, Sb, Te and Bi between monosulfide solid solution and sulfide melt—Application to magmatic sulfide deposits. Geochimica et Cosmochimica Acta 74, 6174–6179.

Le Maitre, R.W., Streckeisen, A., Zanettin, B., et al. (Eds), 2002. In: Igneous Rocks. A Classification and Glossary of Terms. Recommendations of the International Union of Geological Sciences Subcommission on the Systematics of Igneous Rocks. Cambridge University Press, Cambridge, p. 236.

McDonough, W.F., Sun, S.-S., 1995. The composition of the Earth. Chemical Geology 120, 223–253.

Mutanen, T., 1997. Geology and ore petrology of the Akanvaara and Koitelainen mafic layered intrusions and the Keivitsa-Satovaara layered complex, northern Finland. Geological Survey of Finland, Bulletin. 395, p. 233.

Mutanen, T., Huhma, H., 2001. U-Pb geochronology of the Koitelainen, Akanvaara and Keivitsa mafic layered intrusions and related rocks. Geological Survey of Finland. Special Paper 33, 229–246.

Nisbet, E.G., Cheadle, M.J., Arndt, N.T., Bickle, M.J., 1993. Constraining the potential temperature of the Archaean mantle: a review of the evidence from komatiites. Lithos 30, 291–307.

Roeder, P.L., Emslie, R.F., 1970. Olivine-liquid equilibrium. Contributions to Mineralogy and Petrology 29, 275–289.

Yang, S.-H., Maier, W.D., Hanski, E.J., et al., 2013. Origin of ultra-nickeliferous olivine in the Kevitsa Ni-Cu-PGE-mineralised intrusion, northern Finland. Contributions to Mineralogy and Petrology 166, 81–95.